

CHAPTER 6

NUMERICAL WORK

6.1 Introduction

This chapter presents the sequential and parallel results of the experiments conducted using various schemes under consideration for 1-D, 2-D Parabolic and Bio-Heat Equations with similar sequential and parallel results for 1-D, 2-D and 3-D Telegraphic Equations. Approximation solutions were compared to that of other alternating methods for the Parabolic and Telegraphic Equations. The acceleration parameter was chosen to provide the most rapid convergence. Unless otherwise stated the convergence criterion was taken as $eps = 10^{-4}$. The parallel schemes were implemented using MPI and PVM message passing along with C programming language. The schemes used in this Chapter are the schemes treated in Chapters 3, 4 and 5.

6.2 Sequential Results for 1-D Parabolic & Bio-Heat Equations

The 1-D problem considered was taken from (Saulev (1964),) given as

$$\frac{\partial U}{\partial t} = \frac{\partial^2 U}{\partial x^2}, \quad \text{for } 0 < x < 1, \quad 0 < t < T$$

$$U(x,0) = f(x), \quad 0 \leq x \leq 1$$

$$U(0,t) = g_o(t), \quad 0 < t \leq T$$

$$U(1,t) = g_1(t), \quad 0 < t \leq T$$

and subject to initial condition

$$U(x,0) = 4x(1-x) \quad 0 \leq x \leq 1 \quad (6.1)$$

and the boundary conditions

$$U(0,t) = U(1,t) = 0 \quad t \geq 0. \quad (6.2)$$

The exact solution was given by

$$U(x,t) = \frac{32}{\pi^2} \sum_{k=1,(2)}^{\infty} \frac{1}{k^3} e^{-\pi^2 k^2 t} \sin(k\pi x) \quad (6.3)$$

in this experiment, the values of $U(x_i, t)$ where $i = 1$ and m , were taken to satisfy the exact solution Eq. (6.3). An energy balance for a control volume of tissue with volumetric blood flow and metabolism yields the Bio-Heat equation given by (Pennes 1948 and Deng & Liu 2002). We consider the 1-D Bio-Heat equation of the form:

$$\frac{\partial U}{\partial t} = c \left(\frac{\partial^2 U}{\partial x^2} \right) + bU - bU^*. \quad (6.4)$$

The boundary condition and initial condition posed are:

$$U(0,t) = 0, \quad U(1,t) = 0 \quad (6.5)$$

$$U(x,0) = 0.7(1+3x), \quad 0 \leq x \leq 1 \quad (6.6)$$

The values of the physical properties in our test cases are chosen to be $\rho = 1000 \text{ kg/m}^3$, $c = c_b = 4200 \text{ J/kg}^\circ\text{C}$, $\omega_b = 0.5 \text{ kg/m}^3$, the step increase of the temperature is set to be $U_o = 12^\circ\text{C}$.

Table 6.1 Sequential results for 1-D Parabolic Equation with various schemes

Absolute error of numerical solutions, $\lambda = 0.5$, $t = 0.25$, $\Delta t = 0.005$, $\Delta x = 0.1$, $eps = 10^{-4}$

X	method	0.1	0.2	0.3	0.4	0.5	0.6	0.7	0.8	0.9	Av. Abs. Err	RMS*	It.
GS		8.58x10 ⁻³	5.82x10 ⁻²	6.92x10 ⁻³	8.06x10 ⁻³	7.11x10 ⁻²	8.34x10 ⁻²	8.16x10 ⁻²	7.69x10 ⁻³	7.36x10 ⁻²	3.99x10 ⁻¹	3.08x10 ⁻³	7
SOR		6.65x10 ⁻³	4.60x10 ⁻²	4.72x10 ⁻³	7.28x10 ⁻³	6.24x10 ⁻²	7.57x10 ⁻²	7.02x10 ⁻²	6.57x10 ⁻³	6.84x10 ⁻²	3.48x10 ⁻¹	2.39x10 ⁻³	5
IADE-DY		7.53x10 ⁻⁴	1.36x10 ⁻³	8.50x10 ⁻⁵	9.74x10 ⁻⁴	1.71x10 ⁻³	2.05x10 ⁻³	1.97x10 ⁻³	1.52x10 ⁻³	8.00x10 ⁻⁴	1.12x10 ⁻²	1.93x10 ⁻⁶	3
IADE-MF		5.37x10 ⁻⁴	1.02x10 ⁻³	1.41x10 ⁻³	1.65x10 ⁻³	1.74x10 ⁻³	1.65x10 ⁻³	1.41x10 ⁻³	1.02x10 ⁻⁴	5.38x10 ⁻⁴	1.22x10 ⁻³	1.68x10 ⁻⁶	3
IADE 4 th order	-	2.61x10 ⁻⁷	2.98x10 ⁻⁷	5.89x10 ⁻⁶	2.12x10 ⁻⁶	1.09x10 ⁻⁷	7.54x10 ⁻⁷	5.77x10 ⁻⁷	-	1.12x10 ⁻⁶	4.47x10 ⁻¹²	2	
AGE 4 th order	-	2.54x10 ⁻⁷	2.61x10 ⁻⁷	5.65x10 ⁻⁶	2.04x10 ⁻⁶	1.03x10 ⁻⁷	7.27x10 ⁻⁷	5.51x10 ⁻⁷	-	1.07x10 ⁻⁶	4.12x10 ⁻¹²	2	
EXACT SOLN		2.70461 x10 ⁻²	5.14447 x10 ⁻²	7.08075 x10 ⁻²	8.32392 x10 ⁻²	8.7522 x10 ⁻²	8.323992 x10 ⁻²	7.08075 x10 ⁻²	5.14447 x10 ⁻²	2.70461 x10 ⁻²	-	-	-

Table 6.2 Sequential results for 1-D Bio-Heat Equation with various schemes

<i>Method</i>	<i>GS</i>	<i>SOR</i>	<i>IADE-DY</i>	<i>IADE-MF</i>	<i>IADE</i>	<i>4th AGE</i>
<i>4th order</i>						
<i>Av. Abs.</i>						
<i>Err.</i>	4.52×10^{-2}	3.98×10^{-2}	2.63×10^{-3}	2.47×10^{-4}	3.44×10^{-7}	3.11×10^{-7}
<i>RMS</i>	4.39×10^{-4}	3.28×10^{-4}	2.54×10^{-7}	2.28×10^{-7}	5.82×10^{-13}	5.43×10^{-13}
<i>It</i>	9	7	5	4	3	3
Δx	1×10^{-1}	1×10^{-1}				
Δt	5×10^{-3}	5×10^{-3}				
λ	5×10^{-1}	5×10^{-1}				
t	2.5×10^{-1}	2.5×10^{-1}				
<i>eps</i>	1×10^{-4}	1×10^{-4}				

6.3 Parallel Results for 1-D Parabolic and Bio-Heat Equations

Here, we present parallel results for various schemes under consideration using MPI and PVM for various mesh sizes for the 1-D Parabolic and Bio-Heat Equations. Table 6.3 shows various performance timing for 300 meshes for the Parabolic case, while Fig. 6.1 to 6.8 show the parallel performance for 100 to 300 meshes on MPI and PVM platform for Parabolic and Bio-Heat case respectively. From Table 6.3, we can see that the master time T_M is constant when the number of processors increases for a given grid size and number of sub-domains. The master program is responsible for (1) sending updated variables to slaves (T_1), (2) assigning task to slaves (T_2), (3) waiting for the slaves to execute tasks (T_3), (4) receiving the results (T_4).

Table 6.3 Parallel Performance for various schemes with MPI and PVM for 300 mesh
 (1 –D Parabolic case)

		PVM				MPI			
<i>Scheme</i>	<i>N</i>	<i>T_w</i>	<i>T_m</i>	<i>T_{sd}</i>	<i>S_{par}</i>	<i>E_{par}</i>	<i>N</i>	<i>S_{par}</i>	<i>E_{par}</i>
GS	1	258.6	13.8	9.3	1.000	1.000	1	1.000	1.000
	2	231.2	13.8	9.1	1.431	0.716	2	1.624	0.898
	6	193.5	13.6	9.1	1.728	0.288	6	1.813	0.302
	8	168.7	13.6	9.1	2.108	0.264	8	2.296	0.287
	10	118.2	13.6	9.1	2.624	0.262	10	2.865	0.287
	12	98.7	13.6	9.1	2.938	0.245	12	3.208	0.267
	14	85.6	13.6	9.1	3.382	0.242	14	3.468	0.248
	16	82.4	13.6	9.1	3.764	0.235	16	3.861	0.241
SOR	1	279.4	14.5	10.7	1.000	1.000	1	1.000	1.000
	2	256.8	14.3	10.4	1.528	0.764	2	1.808	0.904
	6	211.4	14.3	10.4	1.876	0.313	6	1.928	0.321
	8	180.2	14.3	10.4	2.284	0.286	8	2.387	0.298
	10	168.4	14.3	10.4	2.721	0.272	10	2.962	0.296
	12	114.6	14.3	10.4	3.084	0.257	12	3.381	0.282
	14	97.7	14.3	10.4	3.574	0.255	14	3.711	0.265
	16	91.5	14.3	10.4	4.012	0.251	16	4.108	0.257
IADE-DY	1	328.4	15.8	11.5	1.000	1.000	1	1.000	1.000
	2	304.7	15.6	11.4	1.612	0.806	4	1.879	0.940
	6	258.6	15.6	11.4	1.928	0.321	6	1.948	0.325
	8	223.8	15.6	11.4	2.408	0.301	8	2.518	0.315
	10	211.3	15.6	11.4	2.896	0.290	10	3.096	0.310
	12	193.7	15.6	11.4	3.286	0.274	12	3.421	0.285
	14	170.8	15.6	11.4	3.714	0.265	14	3.822	0.273
	16	120.5	15.6	11.4	4.208	0.263	16	4.325	0.270
IADE-MF	1	335.7	16.2	11.5	1.000	1.000	1	1.000	1.000
	2	310.2	16	11.4	1.786	0.893	2	1.902	0.951
	6	263.5	16	11.4	2.324	0.387	6	2.424	0.404
	8	235.4	16	11.4	2.589	0.324	8	2.687	0.336

10	228.7	16	11.4	2.949	0.295	10	3.118	0.312
12	203.8	16	11.4	3.398	0.283	12	3.513	0.293
14	180.5	16	11.4	3.826	0.273	14	3.911	0.279
16	130.2	16	11.4	4.311	0.269	16	4.426	0.277
1	361.4	18.8	11.5	1.000	1.000	1	1.000	1.000
2	331.8	18.6	11.4	1.824	0.912	2	1.913	0.957
6	284.6	18.6	11.4	2.463	0.411	6	2.584	0.431
IADE-4th	253.7	18.6	11.4	2.628	0.329	8	2.789	0.349
10	239.6	18.6	11.4	3.256	0.326	10	3.396	0.340
12	212.6	18.6	11.4	3.491	0.291	12	3.611	0.301
14	193.5	18.6	11.4	3.988	0.285	14	4.209	0.301
16	148.6	18.6	11.4	4.538	0.284	16	4.714	0.295
1	386.7	20.1	11.5	1.000	1.000	1	1.000	1.000
2	351.5	20.1	11.4	1.908	0.954	2	1.927	0.964
6	299.3	20	11.4	2.521	0.420	6	2.712	0.452
AGE-4th	271.1	20	11.4	2.714	0.339	8	2.866	0.358
10	248.8	20	11.4	3.318	0.332	10	3.429	0.343
12	229.9	20	11.4	3.521	0.293	12	3.713	0.309
14	211.5	20	11.4	4.029	0.288	14	4.261	0.304
16	169.9	20	11.4	4.604	0.288	16	4.821	0.301

Table 6.4 Effectiveness of the various schemes with PVM and MPI for 300 mesh size

(1-D Parabolic case)

	N	PVM T(s)	L_n	MPI T(s)	L_n
GS	1	201.9	0.50	181.7	0.55
	2	141.1	0.51	111.9	0.80
	6	116.8	0.25	100.2	0.30
	8	95.8	0.28	79.1	0.36
	10	76.9	0.34	63.4	0.45
	12	68.7	0.36	56.6	0.47
	14	59.7	0.41	52.4	0.47
	16	53.6	0.44	47.1	0.51
SOR	1	238.3	0.42	221.6	0.45
	2	155.96	0.49	122.57	0.74
	6	127.0	0.25	114.94	0.28

	8	<i>104.33</i>	0.27	92.84	0.32
	10	<i>87.58</i>	0.31	74.8	0.40
	12	<i>77.27</i>	0.33	65.54	0.43
	14	<i>66.68</i>	0.38	59.71	0.44
	16	<i>59.40</i>	0.42	53.94	0.48
<hr/>					
<i>IADE-DY</i>	1	<i>322.6</i>	0.31	307.4	0.33
	2	<i>200.12</i>	0.40	163.60	0.57
	6	<i>167.32</i>	0.19	157.80	0.21
	8	<i>133.97</i>	0.22	122.08	0.26
	10	<i>114.40</i>	0.26	99.29	0.31
	12	<i>98.17</i>	0.28	89.86	0.32
	14	<i>86.86</i>	0.31	80.43	0.34
	16	<i>76.66</i>	0.34	71.08	0.38
<hr/>					
<i>IADE-MF</i>	1	<i>366.1</i>	0.27	324.9	0.31
	2	<i>204.98</i>	0.44	170.82	0.56
	6	<i>157.53</i>	0.25	134.03	0.30
	8	<i>141.41</i>	0.23	120.92	0.28
	10	<i>124.14</i>	0.24	104.20	0.30
	12	<i>107.74</i>	0.26	92.49	0.32
	14	<i>95.69</i>	0.29	83.07	0.34
	16	<i>84.92</i>	0.32	73.41	0.38
<hr/>					
<i>IADE-4th</i>	1	<i>421.8</i>	0.24	409.5	0.24
	2	<i>231.25</i>	0.39	214.06	0.45
	6	<i>171.25</i>	0.24	158.48	0.27
	8	<i>160.50</i>	0.20	146.83	0.24
	10	<i>129.55</i>	0.25	120.58	0.28
	12	<i>120.82</i>	0.24	113.40	0.27
	14	<i>105.77</i>	0.27	97.29	0.31
	16	<i>92.95</i>	0.31	86.87	0.34
<hr/>					
<i>AGE-4th</i>	1	<i>487.6</i>	0.19	496.9	0.20
	2	<i>240.51</i>	0.35	257.86	0.37
	6	<i>174.55</i>	0.20	183.22	0.25
	8	<i>159.9</i>	0.18	173.38	0.21
	10	<i>125.08</i>	0.21	144.91	0.24
	12	<i>116.06</i>	0.20	133.83	0.23
	14	<i>97.47</i>	0.22	116.62	0.26
	16	<i>81.37</i>	0.26	103.07	0.29

Table 6.5 Performance Improvement for 1-D Parabolic with various schemes.

N	PVM T(s)							(%)		
	GS	SOR	IADE -DY	IADE -MF	IAD E- 4 TH	AGE -4 TH	GS+SO R	IADE- DY+IA DE-MF	IADE- 4 TH + AGE-4 TH	SOR+ AGE-4 TH
1	201.9	238.3	322.6	366.1	421.8	519.2	15.3	11.9	18.8	54.1
2	141.1	155.9	200.1	204.9	231.3	272.0	9.5	2.4	15.0	42.7
6	116.8	127.0	167.3	177.5	171.3	205.9	8.0	5.8	16.8	38.3
8	95.8	104.3	133.9	141.4	160.5	191.3	8.2	5.3	16.1	45.5
10	76.9	87.6	111.4	124.1	129.6	156.5	12.2	10.3	17.2	44
12	68.7	77.27	98.17	107.7	120.8	147.5	11.1	8.9	18.1	47.6
14	59.7	66.7	86.9	95.7	105.8	128.9	10.5	9.2	17.9	48.3
16	53.6	59.4	76.7	84.9	92.95	112.8	9.8	9.7	17.6	47.3

Table 6.6 Performance Improvement for 300 mesh size 1-D Parabolic with various schemes.

N	MPI T(s)							(%)		
	GS	SOR	IADE -DY	IADE -MF	IAD E- 4 TH	AGE -4 TH	GS+SO R	IADE- DY+IA DE-MF	IADE- 4 TH + AGE-4 TH	SOR+ AGE-4 TH
1	181.7	221.6	307.4	324.9	409.5	496.9	18.0	5.4	17.6	55.4
2	111.9	122.6	163.6	170.8	214.1	257.9	8.7	4.2	17.0	52.5
6	100.2	114.9	157.8	164.0	158.5	183.2	12.8	3.8	13.5	37.3
8	79.1	92.84	122.1	138.9	146.8	173.4	14.8	12.1	15.3	46.5
10	63.4	74.8	99.3	104.2	120.6	144.9	15.2	4.7	16.8	48.4
12	56.6	65.54	89.9	92.5	113.4	133.8	13.6	2.8	15.3	51.0
14	52.4	59.7	80.4	83.1	97.3	116.6	12.2	3.2	16.6	48.8
16	47.1	53.9	71.1	73.4	86.9	103.1	12.7	3.2	15.7	47.7

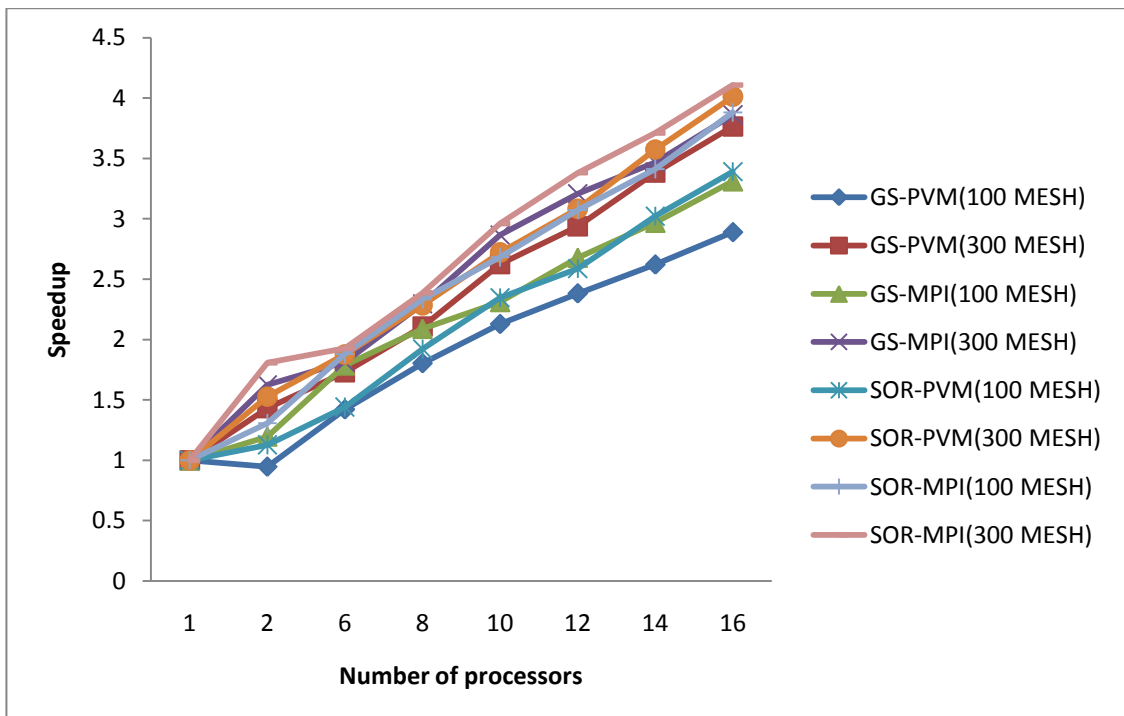


Fig. 6.1 Speed-up of GS, SOR ($\omega = 1.25$) for 100 & 300 meshes with MPI and PVM (1-D Parabolic)

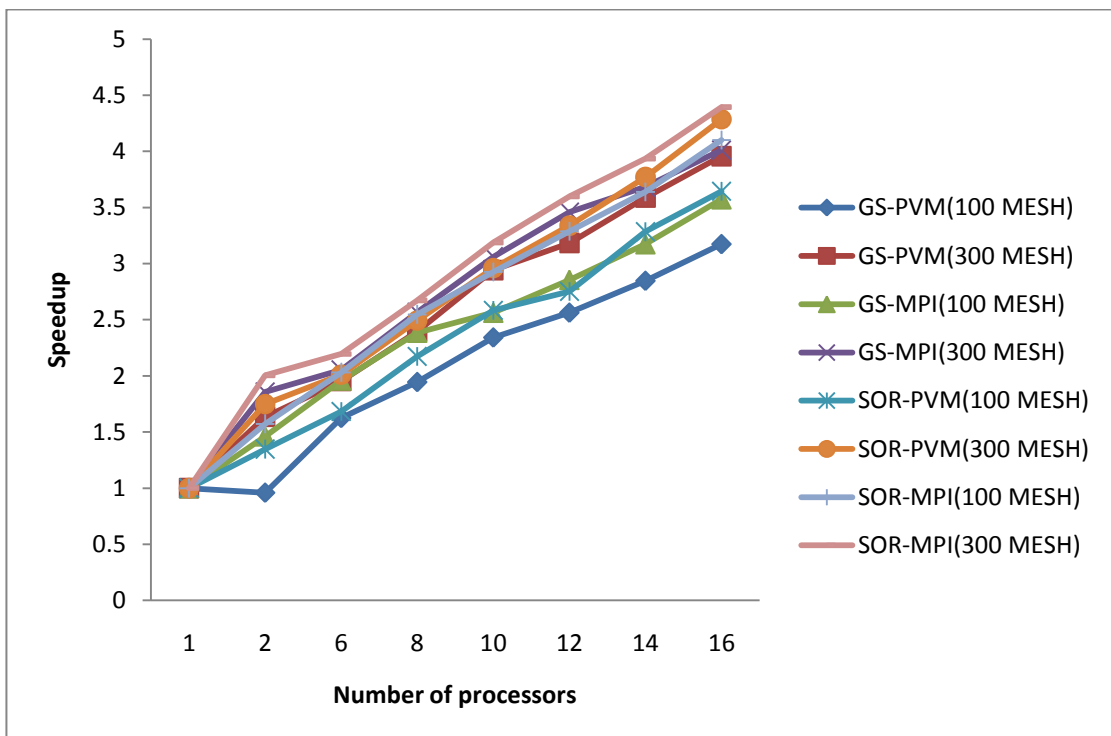


Fig. 6.2 Speed-up of GS & SOR ($\omega = 1.25$) for 100 & 300 meshes with MPI and PVM (1-D Bio-Heat)

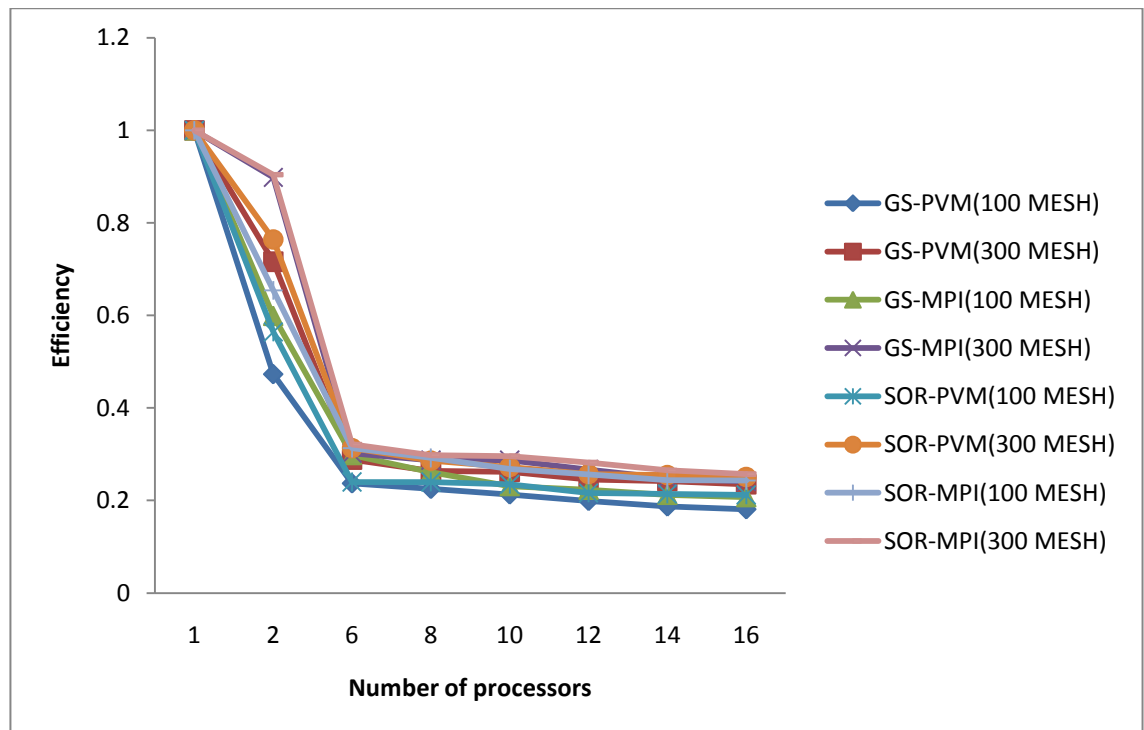


Fig. 6.3 Efficiency of GS & SOR ($\omega = 1.25$) for 100 & 300 meshes with MPI and PVM

(1-D Parabolic)

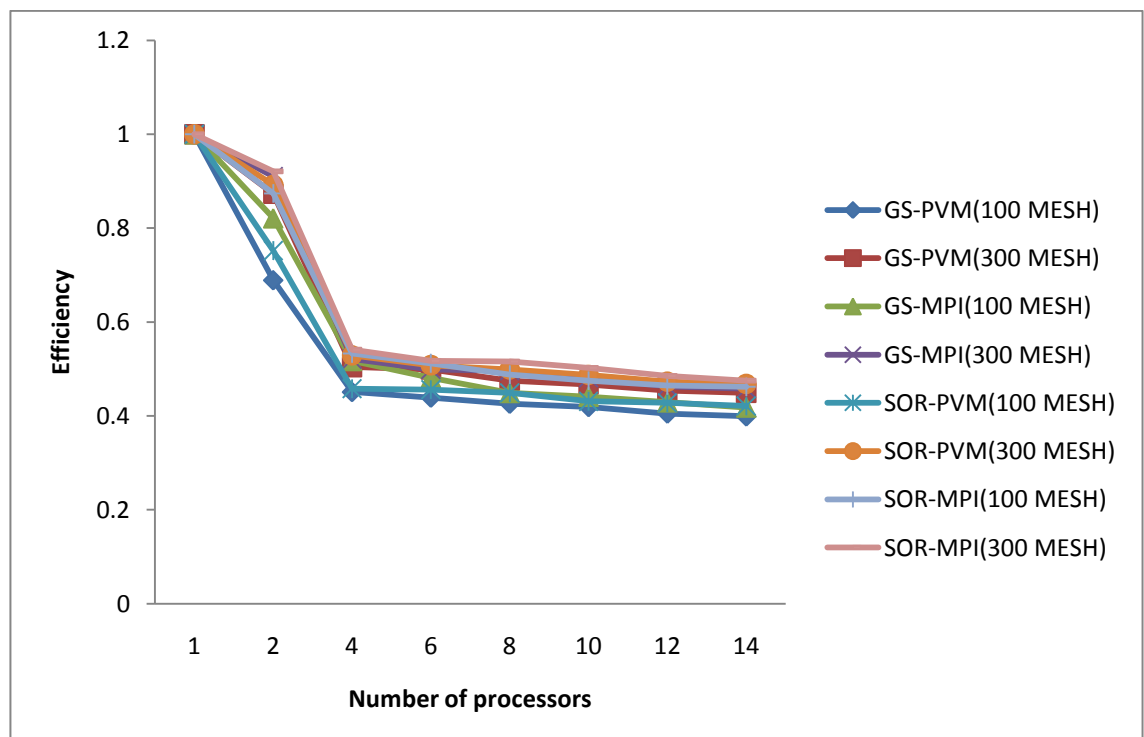


Fig. 6.4 Efficiency of GS & SOR ($\omega = 1.25$) for 100 & 300 meshes with MPI and PVM

(1-D Bio-Heat)

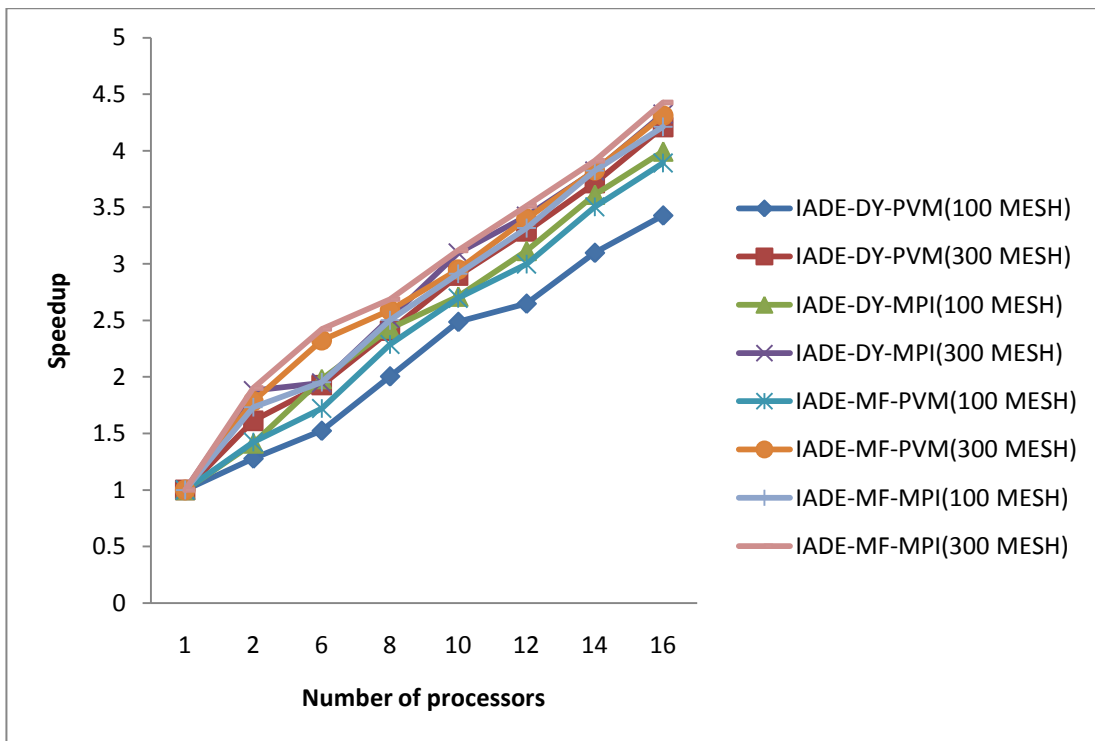


Fig. 6.5 Speedup of IADE-DY & IADE-MF for 100 & 300 meshes with MPI and PVM
(1-D Parabolic)

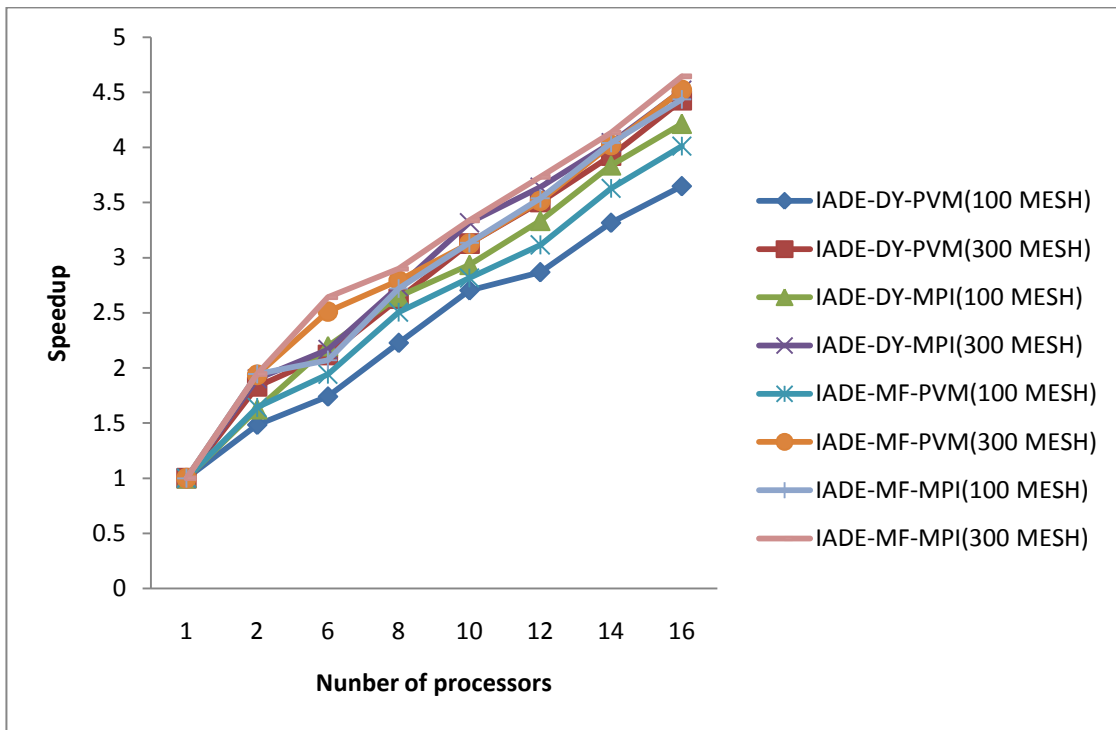


Fig. 6.6 Speedup of IADE-DY & IADE-MF for 100 & 300 meshes with MPI and PVM
(1-D Bio-Heat)

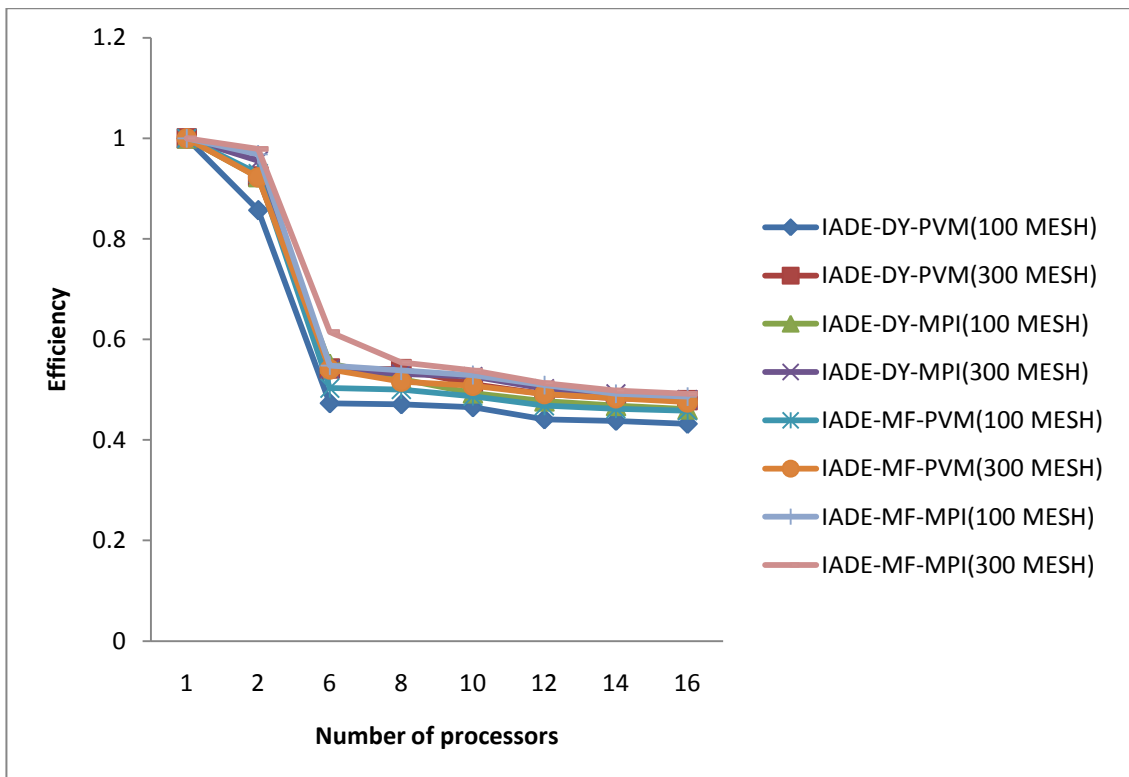


Fig. 6.7 Efficiency of IADE-DY & IADE-MF for 100 & 300 meshes with MPI and PVM (1-D Bio-Heat)

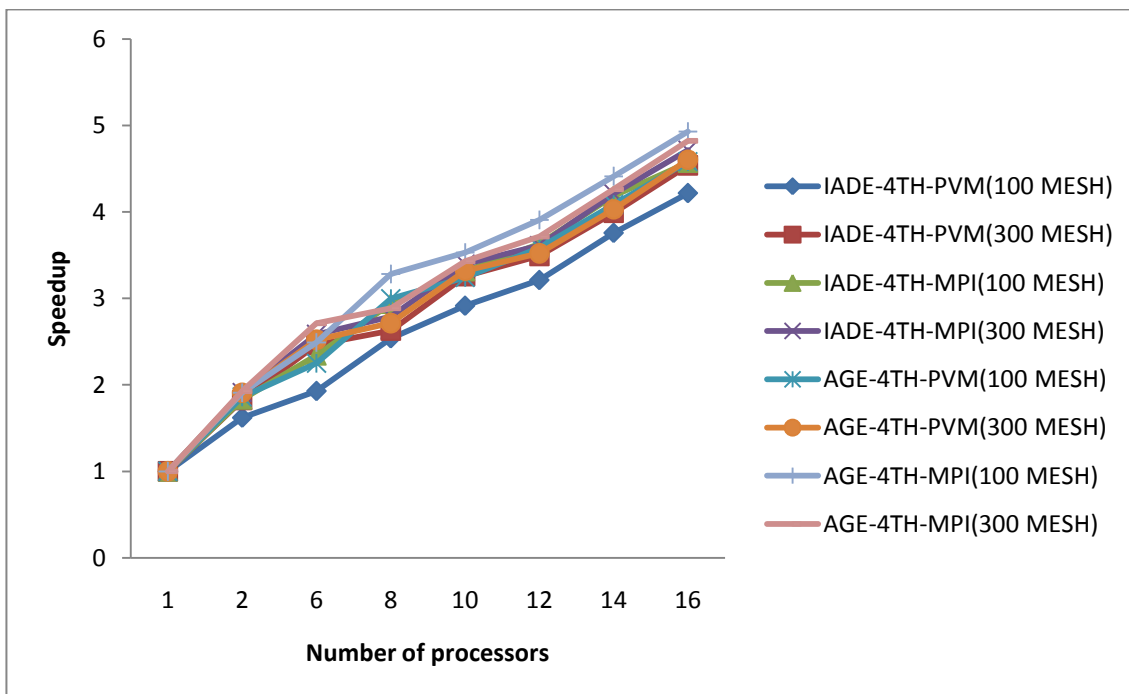


Fig. 6.8 Speedup of IADE-DY-4th & AGE-4th for 100 & 300 meshes with MPI and PVM (1-D Parabolic)

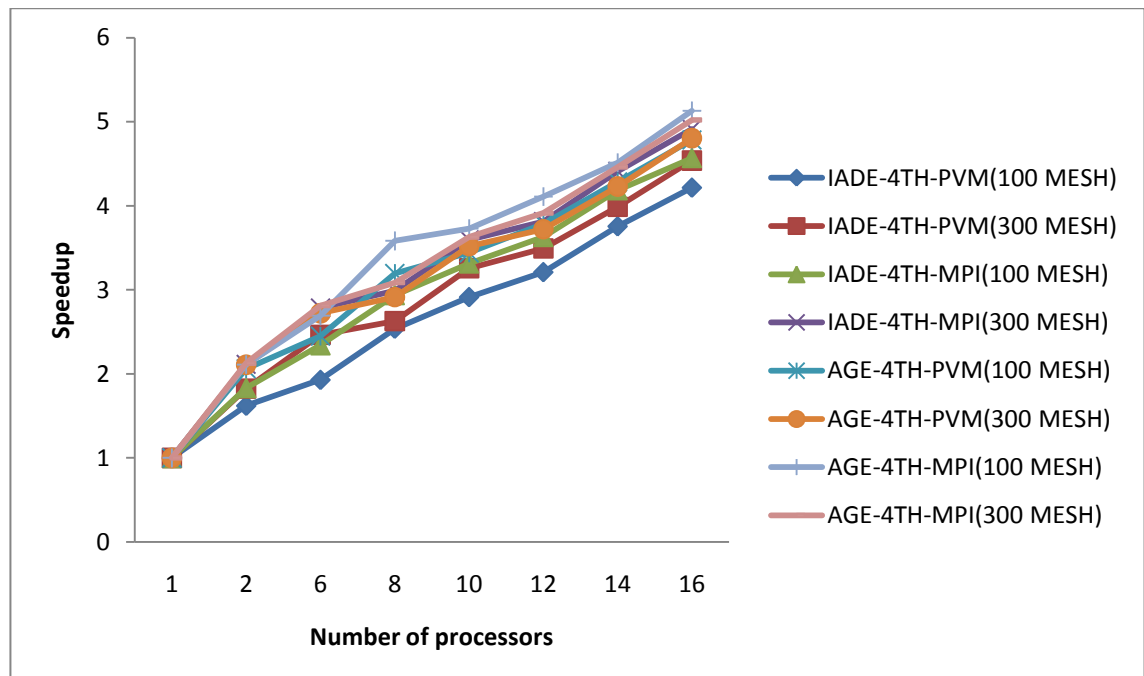


Fig. 6.9 Speedup of IADE-DY-4th & AGE-4th for 100 & 300 meshes with MPI and PVM (1-D Bio-Heat)

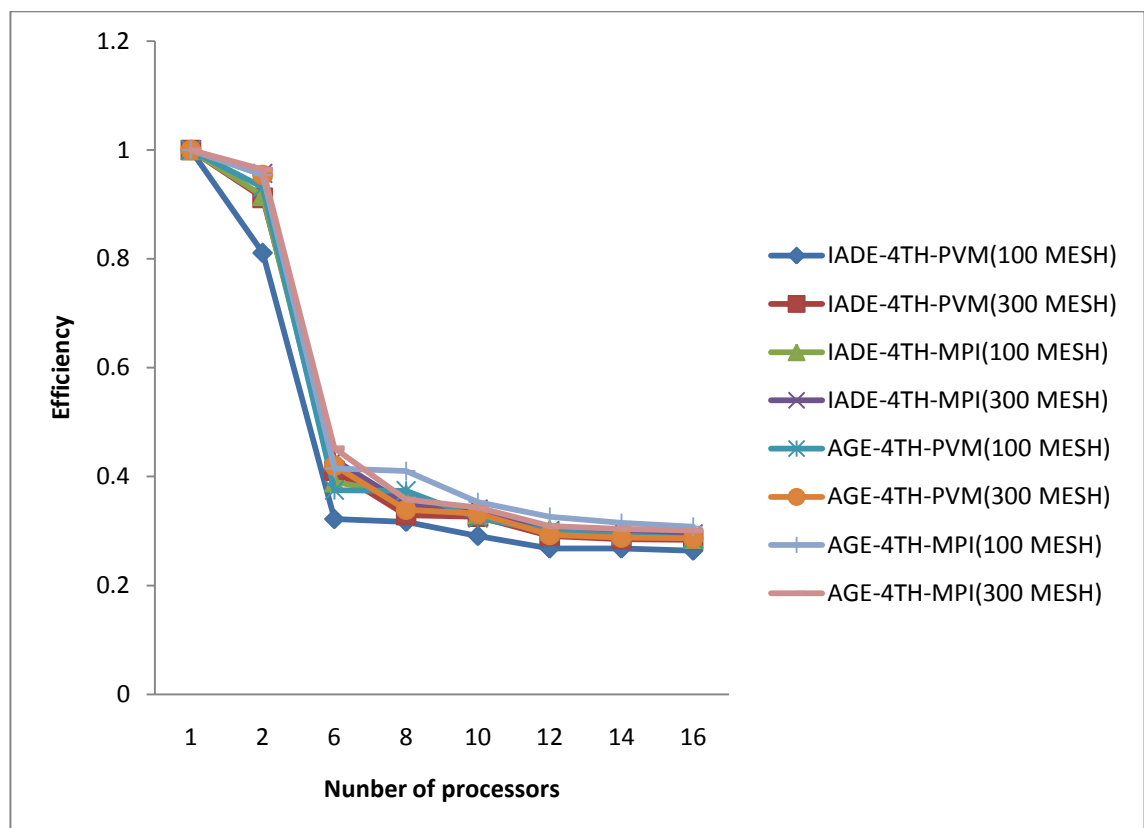


Fig. 6.10 Efficiency of IADE-DY-4th & AGE-4th for 100 & 300 meshes with MPI and PVM (1-D Parabolic)

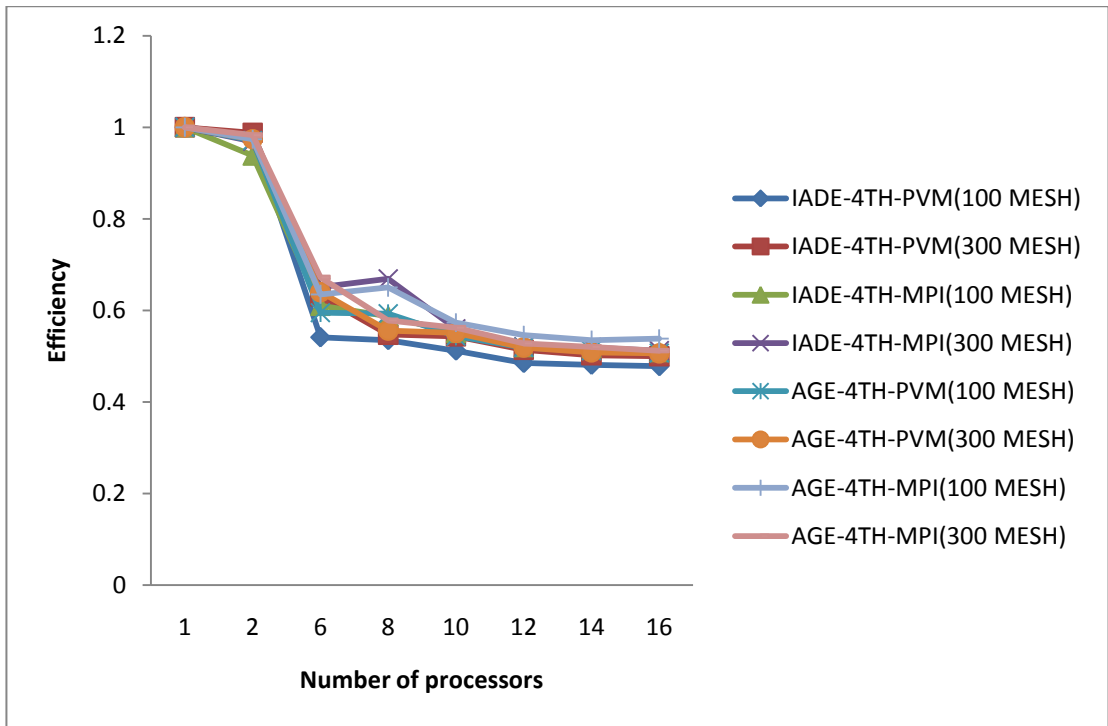


Fig. 6.11 Efficiency of IADE-DY-4th & AGE-4th for 100 & 300 meshes with MPI and PVM (1-D Bio-Heat)

6.4 Sequential Results for 2-D Parabolic and Bio-Heat Equations

The algorithms were tested on 2-D Parabolic Equation and the numerical results of the various schemes are tabulated in the Table 6.7 below. We consider the PDE by (Johnson & Riess (1982)) given as

$$\frac{\partial u(x, y, t)}{\partial t} = \alpha^2 \left[\frac{\partial^2 u(x, y, t)}{\partial x^2} + \frac{\partial^2 u(x, y, t)}{\partial y^2} \right] \quad 0 \leq x \leq 2, 0 \leq y \leq 1, t \geq 0.$$

The boundary condition and initial condition posed are:

$$\begin{cases} u(0, y, t) = 0 \\ u(2, y, t) = 0 \\ u(x, 0, t) = 0 \\ u(x, 1, t) = 0 \end{cases} \quad (6.7)$$

$$u(x, y, 0) = \sin(\pi x) \sin(2\pi y) \quad (0 \leq x \leq 1, 0 \leq y \leq 1) . \quad (6.8)$$

The exact solution is given by

$$u(x, y, t) = e^{-5\pi^2 t} \sin(2\pi x) \sin(\pi y).$$

We evaluated the schemes on Bio-Heat Equation given by (Jennifer et. al. 2002 and Dai & Zhang 2002)) and Table 6.8 shows the sequential computational results. The 2-D Bio-Heat equation of the form:

$$\frac{\partial U}{\partial t} = c \left(\frac{\partial^2 U}{\partial x^2} + \frac{\partial^2 U}{\partial y^2} \right) - bU + bU^\oplus, \quad (6.9)$$

The boundary condition and initial condition posed are:

$$\left. \begin{array}{l} U(0, y, t) = 0 \\ U(1, y, t) = 0 \\ U(x, 0, t) = 0 \\ U(x, 1, t) = 0 \end{array} \right\} \quad t \geq 0 \quad (6.10)$$

$$U(x, y, 0) = x(\pi - x - 1)y(\pi - y - 1) \quad (0 \leq x \leq 1, 0 \leq y \leq 1)$$

The cell size was chosen as $\Delta x = \Delta y$. The values of the physical properties in our test cases are chosen to be $\rho = 1000 \text{ kg/m}^3$, $c = c_b = 4200 \text{ J/kg}^\circ\text{C}$, $\omega_b = 0.5 \text{ kg/m}^3$, temperature is set to be $U_o = 12^\circ\text{C}$.

Table 6.7 Sequential results for 2-D Parabolic Equation with various schemes

Absolute error of numerical solutions, $\lambda = 0.5, \Delta x = \Delta y = 0.02, t = 0.0018, \Delta t = 0.0002, r = 1.0, \text{eps} = 10^{-4}, y = 0.02$											
X method	0.02	0.3	0.58	0.86	1.14	1.42	1.7	1.98	Abs. Err	RMS*	It.
GS	4.08x10 ⁻³	5.92x10 ⁻³	6.21x10 ⁻³	8.65x10 ⁻³	8.92x10 ⁻³	8.65x10 ⁻³	6.21x10 ⁻³	5.92x10 ⁻³	6.82x10 ⁻³	4.91x10 ⁻⁵	9
SOR	2.93x10 ⁻³	4.79x10 ⁻³	5.91x10 ⁻³	7.31x10 ⁻³	7.50x10 ⁻³	7.31x10 ⁻³	5.91x10 ⁻³	4.79x10 ⁻³	5.81x10 ⁻³	3.20x10 ⁻⁵	7
IADE-DY											
	2.31x10 ⁻³	4.23x10 ⁻³	5.52x10 ⁻³	6.21x10 ⁻³	6.43x10 ⁻³	6.21x10 ⁻³	5.52x10 ⁻³	4.23x10 ⁻³	5.08x10 ⁻³	2.47x10 ⁻⁵	5
MF-DS											
	5.58x10 ⁻⁶	2.14x10 ⁻⁵	1.73x10 ⁻⁵	1.62x10 ⁻⁵	2.21x10 ⁻⁵	6.35x10 ⁻⁶	2.42x10 ⁻⁵	1.54x10 ⁻⁶	1.43x10 ⁻⁵	2.71x10 ⁻¹⁰	4
AGE											
	1.45x10 ⁻⁶	9.88x10 ⁻⁶	5.28x10 ⁻⁶	7.9x10 ⁻⁶	8.24x10 ⁻⁶	4.82x10 ⁻⁶	1.0x10 ⁻⁵	1.28x10 ⁻⁶	6.11x10 ⁻⁶	3.54x10 ⁻¹¹	4
EXACT											
SOLN	7.2008	5.46416	-2.76785	-4.42688	4.42688	2.76785	-5.46416	-7.2008	-	-	-
	x10 ⁻³	x10 ⁻²	x10 ⁻³								

Table 6.8 Sequential results for 2-D Bio-Heat Equation with various schemes

Method	GS	SOR	IADE-DY	MF-DS	AGE
Av. Abs.					
Err.	10.5×10^{-4}	8.7×10^{-4}	5.8×10^{-5}	4.2×10^{-6}	5.1×10^{-7}
RMS	5.6×10^{-4}	4.3×10^{-7}	5.6×10^{-6}	4.7×10^{-7}	5.2×10^{-13}
It	11	9	7	5	5
Δx	1×10^{-1}	1×10^{-1}	1×10^{-1}	1×10^{-1}	1×10^{-1}
Δt	2×10^{-4}	2×10^{-4}	2×10^{-4}	2×10^{-4}	2×10^{-4}
λ	5×10^{-1}	5×10^{-1}	5×10^{-1}	5×10^{-1}	5×10^{-1}
t	1.8×10^{-3}	1.8×10^{-3}	1.8×10^{-3}	1.8×10^{-3}	1.8×10^{-3}
eps	1×10^{-4}	1×10^{-4}	1×10^{-4}	1×10^{-4}	1×10^{-4}

6.5 Parallel Results for 2-D Parabolic and Bio-Heat Equations

The speedup and efficiency obtained for various grid sizes for the PVM and MPI implementation are given in the figures below and Table 6.9 list the values for 300 x 300 mesh sizes for 2-D Parabolic case.

Table 6.9: 300 x 300 mesh sizes using various schemes

PVM						MPI			
Scheme	N	T_w	T_m	T_{sd}	S_{par}	E_{par}	N	S_{par}	E_{par}
GS	1	528.9	33.6	8.7	1.000	1.000	1	1.000	1.000
	2	496.1	33.4	8.5	1.648	0.824	2	1.67	0.835
	6	413.8	33.4	8.5	2.448	0.408	6	2.481	0.414
	8	378.5	33.4	8.5	3.076	0.385	8	3.196	0.400
	10	321.5	33.4	8.5	3.635	0.364	10	3.765	0.377
	12	252.7	33.4	8.5	4.11	0.343	12	4.278	0.357
	14	210.5	33.4	8.5	4.312	0.308	14	4.788	0.342
	16	189.7	33.4	8.5	4.164	0.260	16	5.024	0.314
SOR	1	685.4	38.6	9.5	1.000	1.000	1	1.000	1.000
	2	536.8	38.5	9.3	1.786	0.893	2	1.798	0.899
	6	482.1	38.5	9.3	2.625	0.438	6	2.658	0.443
	8	413.8	38.5	9.3	3.284	0.411	8	3.476	0.435

	<i>10</i>	386.9	38.5	9.3	4.07	0.407	<i>10</i>	4.24	0.424
	<i>12</i>	251.8	38.5	9.3	4.752	0.396	<i>12</i>	4.926	0.411
	<i>14</i>	210.1	38.5	9.3	5.089	0.364	<i>14</i>	5.572	0.398
	<i>16</i>	189.6	38.5	9.3	5.584	0.349	<i>16</i>	5.976	0.374
<hr/>									
	<i>1</i>	691.8	41.2	9.7	1.000	1.000	<i>1</i>	1.000	1.000
	<i>2</i>	543.7	41	9.6	1.798	0.899	<i>2</i>	1.812	0.906
	<i>6</i>	487.1	41	9.6	2.661	0.444	<i>6</i>	2.685	0.448
<i>ADI</i>	<i>8</i>	408.5	41	9.5	3.46	0.433	<i>8</i>	3.524	0.441
	<i>10</i>	398.8	41	9.5	4.155	0.416	<i>10</i>	4.315	0.432
	<i>12</i>	262.6	41	9.5	4.806	0.401	<i>12</i>	5.082	0.424
	<i>14</i>	208.9	41	9.5	5.474	0.391	<i>14</i>	5.733	0.410
	<i>16</i>	199.3	41	9.5	5.792	0.362	<i>16</i>	6.176	0.386
<hr/>									
	<i>1</i>	702.5	46.3	10.1	1.000	1.000	<i>1</i>	1.000	1.000
	<i>2</i>	556.1	46.2	9.7	1.816	0.908	<i>2</i>	1.822	0.911
<i>IADE-DY</i>	<i>6</i>	491.5	46.2	9.7	2.688	0.448	<i>6</i>	2.715	0.453
	<i>8</i>	412.8	46.2	9.7	3.528	0.441	<i>8</i>	3.564	0.446
	<i>10</i>	401.9	46.2	9.7	4.305	0.431	<i>10</i>	4.39	0.439
	<i>12</i>	271.6	46.2	9.7	5.07	0.423	<i>12</i>	5.196	0.433
	<i>14</i>	211.5	46.2	9.7	5.719	0.409	<i>14</i>	5.873	0.420
	<i>16</i>	201.4	46.2	9.7	6.296	0.394	<i>16</i>	6.512	0.407
<hr/>									
	<i>1</i>	702.5	51.3	10.1	1.000	1.000	<i>1</i>	1.000	1.000
	<i>2</i>	556.1	51.2	9.7	1.834	0.917	<i>2</i>	1.922	0.961
<i>MF-DS</i>	<i>6</i>	491.5	51.2	9.7	2.728	0.455	<i>6</i>	2.749	0.458
	<i>8</i>	412.8	51.2	9.7	3.671	0.459	<i>8</i>	3.744	0.468
	<i>10</i>	401.9	51.2	9.7	4.396	0.440	<i>10</i>	4.51	0.451
	<i>12</i>	271.6	51.2	9.7	5.108	0.426	<i>12</i>	5.268	0.439
	<i>14</i>	211.5	51.2	9.7	5.827	0.416	<i>14</i>	5.95	0.425
	<i>16</i>	201.4	51.2	9.7	6.374	0.398	<i>16</i>	6.544	0.409
<hr/>									
	<i>1</i>	702.5	54.2	10.1	1.000	1.000	<i>1</i>	1.000	1.000
	<i>2</i>	686.1	54	9.7	1.896	0.948	<i>4</i>	1.933	0.967
<i>AGE</i>	<i>6</i>	591.5	54	9.7	2.889	0.482	<i>6</i>	2.921	0.487
	<i>8</i>	512.8	54	9.7	3.738	0.467	<i>8</i>	3.861	0.483
	<i>10</i>	501.9	54	9.7	4.415	0.442	<i>10</i>	4.568	0.457
	<i>12</i>	471.6	54	9.7	5.188	0.432	<i>12</i>	5.364	0.447

14	411.5	54	9.7	5.906	0.422	14	6.018	0.430
16	361.4	54	9.7	6.495	0.406	16	6.628	0.414

Table 6.10 Effectiveness of the various schemes with PVM and MPI for 300x300 mesh size (Parabolic case)

	N	PVM T(s)	L_n	MPI T(s)	L_n
GS	1	752.4	0.13	718.3	0.14
	2	456.6	0.18	430.1	0.19
	6	307.4	0.13	289.5	0.14
	8	244.6	0.15	224.75	0.18
	10	206.9	0.18	190.8	0.20
	12	183.1	0.19	167.9	0.21
	14	174.5	0.18	150.0	0.23
	16	180.7	0.14	142.97	0.22
SOR	1	876.5	0.11	841.8	0.12
	2	490.8	0.18	468.2	0.19
	6	333.9	0.13	316.7	0.14
	8	266.9	0.15	242.2	0.18
	10	215.4	0.19	198.5	0.21
	12	184.5	0.21	170.9	0.24
	14	172.2	0.21	151.1	0.26
	16	156.9	0.22	140.9	0.27
ADI	1	992.4	0.10	928.7	0.11
	2	551.9	0.16	512.5	0.18
	6	372.9	0.12	345.9	0.13
	8	286.8	0.15	263.5	0.17
	10	238.8	0.17	215.2	0.20
	12	206.5	0.19	182.74	0.23
	14	181.3	0.22	161.9	0.25
	16	171.3	0.21	150.4	0.26
IADE-DY	1	1241.7	0.08	1108.2	0.09
	2	683.8	0.13	608.2	0.15
	6	461.9	0.10	408.2	0.11
	8	351.9	0.13	310.9	0.14
	10	288.4	0.15	252.4	0.17
	12	244.9	0.17	213.3	0.20
	14	217.1	0.19	188.7	0.22
	16	197.2	0.20	170.2	0.24
	1	1508.1	0.07	1312.7	0.08

MF-DS	2	822.3	0.11	682.9	0.14
	6	552.8	0.08	477.5	0.10
	8	410.8	0.11	350.6	0.13
	10	343.1	0.13	291.1	0.15
	12	295.2	0.14	249.2	0.18
	14	258.8	0.16	220.6	0.19
	16	236.6	0.17	200.6	0.20

AGE	1	1933.3	0.05	1798.5	0.06
	2	1019.7	0.09	930.42	0.10
	6	669.19	0.07	615.71	0.08
	8	517.20	0.09	465.81	0.10
	10	437.89	0.10	393.72	0.12
	12	372.65	0.12	335.29	0.13
	14	327.35	0.13	298.85	0.14
	16	297.66	0.14	271.35	0.15

Table 6.11 Performance Improvement for 300x300 2-D Parabolic with various schemes.

N	PVM T(s)						(%)			
	GS	SOR	ADI	IADE	MF-DY	AGE	GS+SOR	ADI+IADE-DY	MF-DS+AGE	AGE+SOR
1	752.4	876.5	992.4	1242	1508	1933	14.2	20.1	22	54.7
2	456.6	490.8	551.9	683.8	822.3	1019	7.0	19.3	19.4	51.9
6	307.4	333.9	372.9	461.9	552.8	669.2	8.0	19.3	17.4	50.1
8	244.6	266.9	288.8	351.9	410.8	517.2	8.4	18.5	20.6	48.4
10	206.9	215.4	238.8	288.4	343.1	437.9	3.9	17.2	21.6	50.9
12	183.1	184.5	206.5	244.9	295.2	372.7	0.8	15.7	20.8	50.5
14	174.5	179.2	181.3	217.1	258.8	327.4	2.6	16.5	20.9	45.3
16	180.7	196.9	171.3	197.2	236.6	297.7	8.3	13.1	20.5	33.8

Table 6.12 Performance Improvement for 300x300 2-D Parabolic with various schemes.

N	MPI T(s)						(%)			
	GS	SOR	ADI	IADE	MF-DY	AGE	GS+SOR	ADI+IADE-DY	MF-DS+AGE	AGE+SOR
1	718.3	841.8	928.7	1108	1313	1799	14.7	16.2	27.0	53.2
2	430.1	468.2	512.5	608.2	683	930.4	8.1	15.7	26.6	49.7
6	289.5	316.7	345.9	408.2	477.5	615.7	8.6	15.3	22.4	48.6
8	224.8	242.2	263.5	310.9	350.6	465.8	7.2	15.2	24.7	48.0
10	190.8	198.5	215.2	252.4	291.1	393.7	3.9	14.7	26.1	49.6
12	167.9	170.9	182.7	213.3	249.2	335.3	1.7	14.3	25.7	49.0
14	150.0	151.1	161.9	188.7	220.6	298.9	0.7	14.2	26.2	49.4
16	142.9	149.9	150.4	170.2	200.6	271.4	4.6	11.6	26.1	44.8

Table 6.13 Slave computational time for 100 iterations as a function of block numbers
for PVM
(2-D Parabolic case)

<i>NI x NJ</i>	<i>B = 50</i>	<i>B = 100</i>	<i>B = 200</i>
<i>100 x 100</i>	589	723	846
<i>200 x 200</i>	1012	1342	1528
<i>300 x 300</i>	1869	2225	2586

Table 6.14 Slave computational time for 100 iterations as a function of block numbers
for MPI
(2-D Parabolic case)

<i>NI x NJ</i>	<i>B = 50</i>	<i>B = 100</i>	<i>B = 200</i>
<i>100 x 100</i>	511	689	803
<i>200 x 200</i>	983	1208	1493
<i>300 x 300</i>	1528	2108	2414

Table 6.15 The number of iteration to achieve a given tolerance of 10^{-4} for a grid of 100
 \times 100 PVM (2-D Parabolic case)

<i>N</i>	<i>B = 50</i>	<i>B = 100</i>	<i>B = 200</i>
<i>1</i>	4528	4912	3208
<i>2</i>	4704	5028	3416
<i>6</i>	4813	5217	3727
<i>8</i>	4984	5308	3921
<i>10</i>	5203	5604	4219
<i>12</i>	5321	5638	4307
<i>14</i>	5408	5673	4321
<i>16</i>	5421	5907	4434

Table 6.16 The number of iteration to achieve a given tolerance of 10^{-4} for a grid of 100
 \times 100
MPI (2-D Parabolic case)

<i>N</i>	<i>B = 50</i>	<i>B = 100</i>	<i>B = 200</i>
<i>1</i>	4243	4718	2948
<i>2</i>	4628	4976	3418
<i>6</i>	4721	5108	3639
<i>8</i>	4797	5211	3741
<i>10</i>	5108	5416	3968
<i>12</i>	5219	5527	4114
<i>14</i>	5337	5599	4225
<i>16</i>	5377	5682	4311

Table 6.17 The number of iteration to achieve a given tolerance of 10^{-4} for a grid of 200 x 200 PVM (2-D Parabolic case)

N	B = 50	B = 100	B = 200
1	5012	5128	3764
2	5247	5389	3824
6	5299	5463	3918
8	5437	5511	4210
10	5558	5793	4328
12	5789	5912	4479
14	5921	5993	4528
16	5921	6037	4611

Table 6.18 The number of iteration to achieve a given tolerance of 10^{-4} for a grid of 200 x 200 MPI (2-D Parabolic case)

N	B = 50	B = 100	B = 200
1	4821	4978	3582
2	4962	4998	3608
6	5108	5224	3773
8	5219	5328	3994
10	5307	5515	4205
12	5438	5708	4324
14	5776	5834	4494
16	5776	5938	4502

Table 6.19 The number of iteration to achieve a given tolerance of 10^{-4} for a grid of 300 x 300 PVM (2-D Parabolic case)

N	B = 50	B = 100	B = 200
1	5343	5734	3912
2	5938	6214	4328
6	6234	6373	4494
8	6432	6498	4528
10	6539	6677	4621
12	6683	6721	4696
14	6878	6808	4701
16	6878	6874	4799

Table 6.20 The number of iteration to achieve a given tolerance of 10^{-4} for a grid of 300 x 300 MPI (2-D Parabolic case)

N	B = 50	B = 100	B = 200
1	5321	5582	3781
2	5911	5987	4084
6	6024	6118	4212
8	6133	6228	4314
10	6341	6393	4582
12	6417	6528	4609

14

6613

6782

4693

16

6621

6811

4724

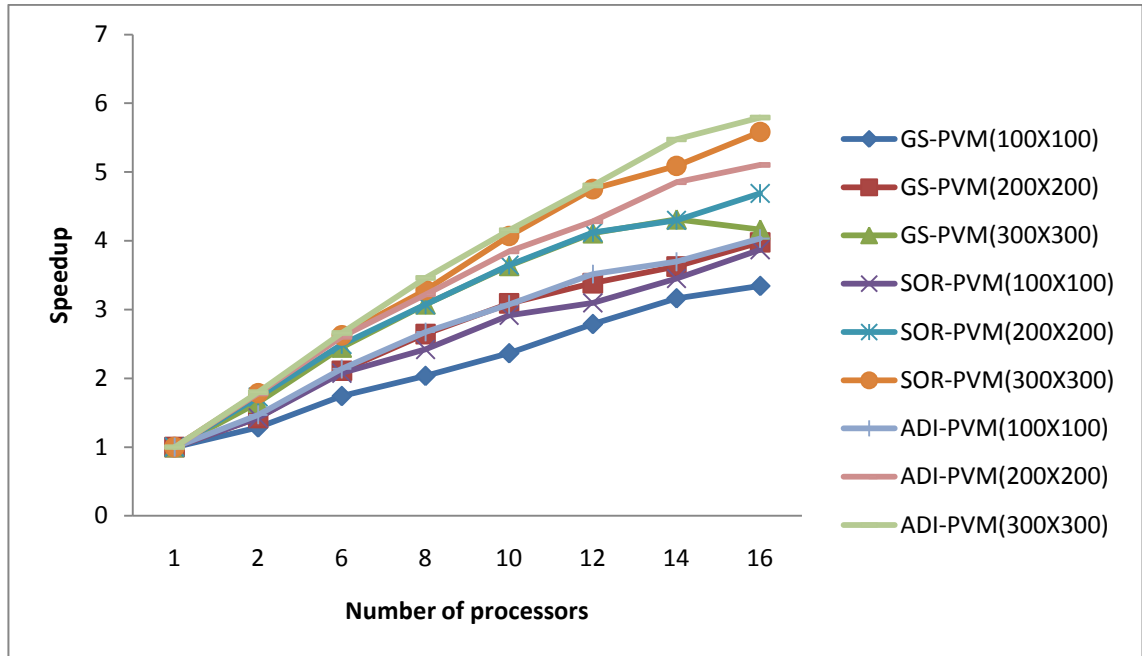


Fig. 6.12 Speedup for 100x100 to 300x300 meshes with PVM (2-D Parabolic)

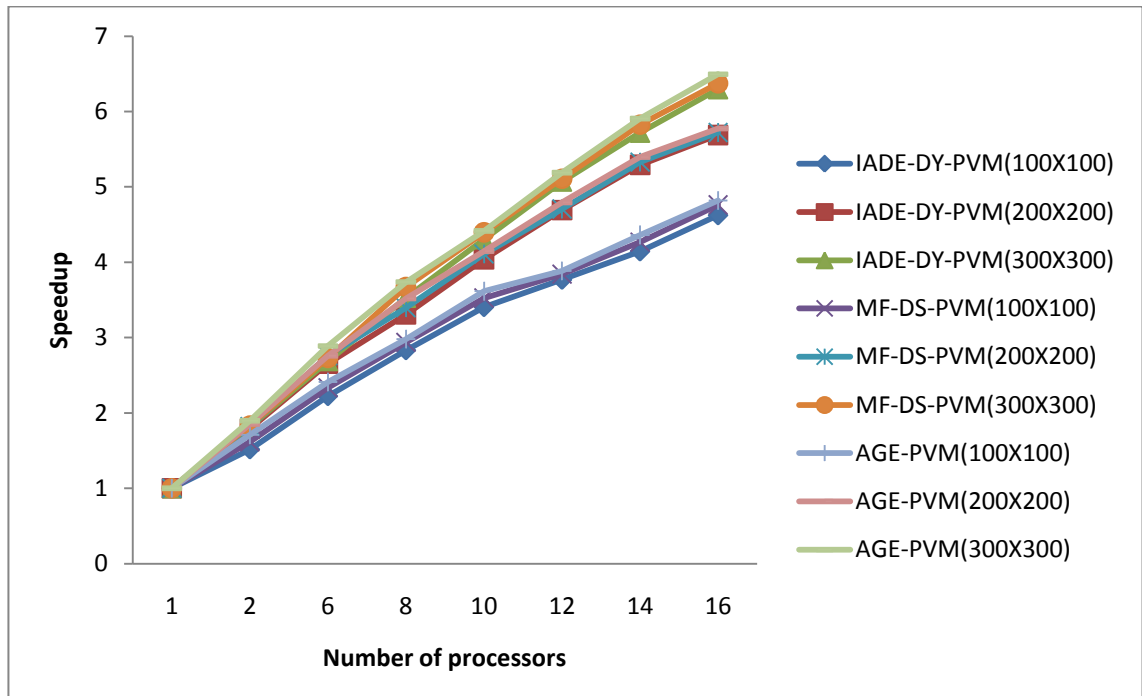


Fig. 6.13 Speedup for 100x100 to 300x300 meshes with PVM (2-D Bio-Heat)

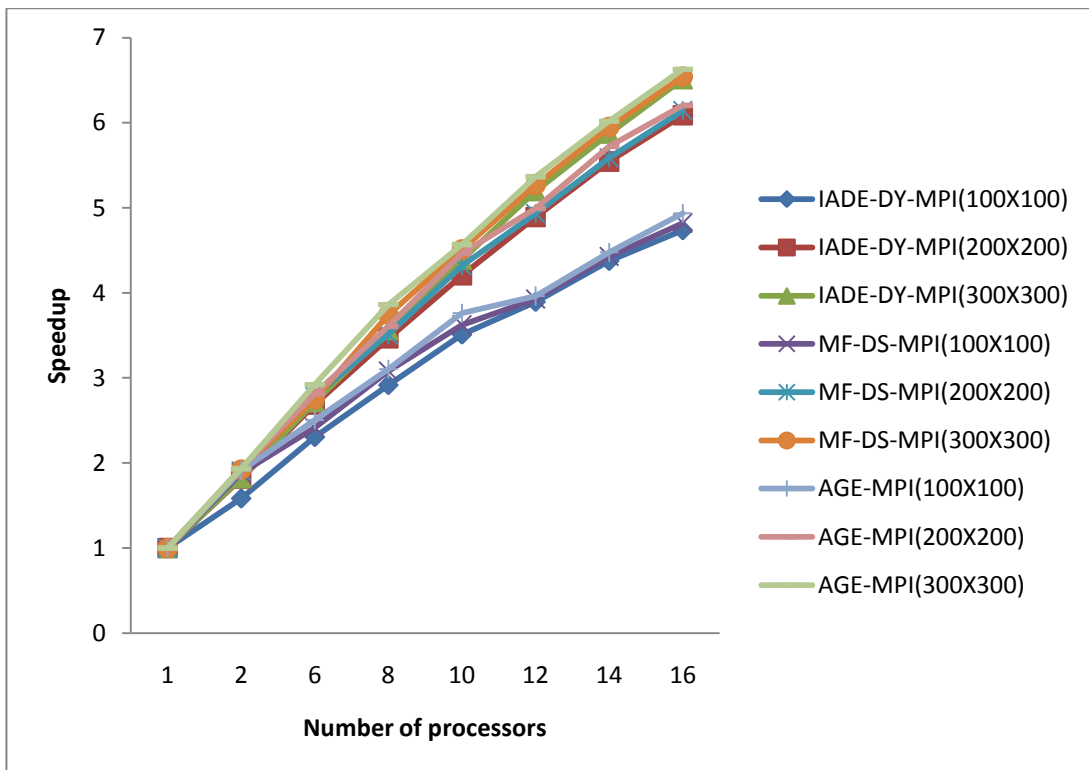


Fig. 6.14 Speedup for 100x100 to 300x300 meshes with MPI (2-D Parabolic)

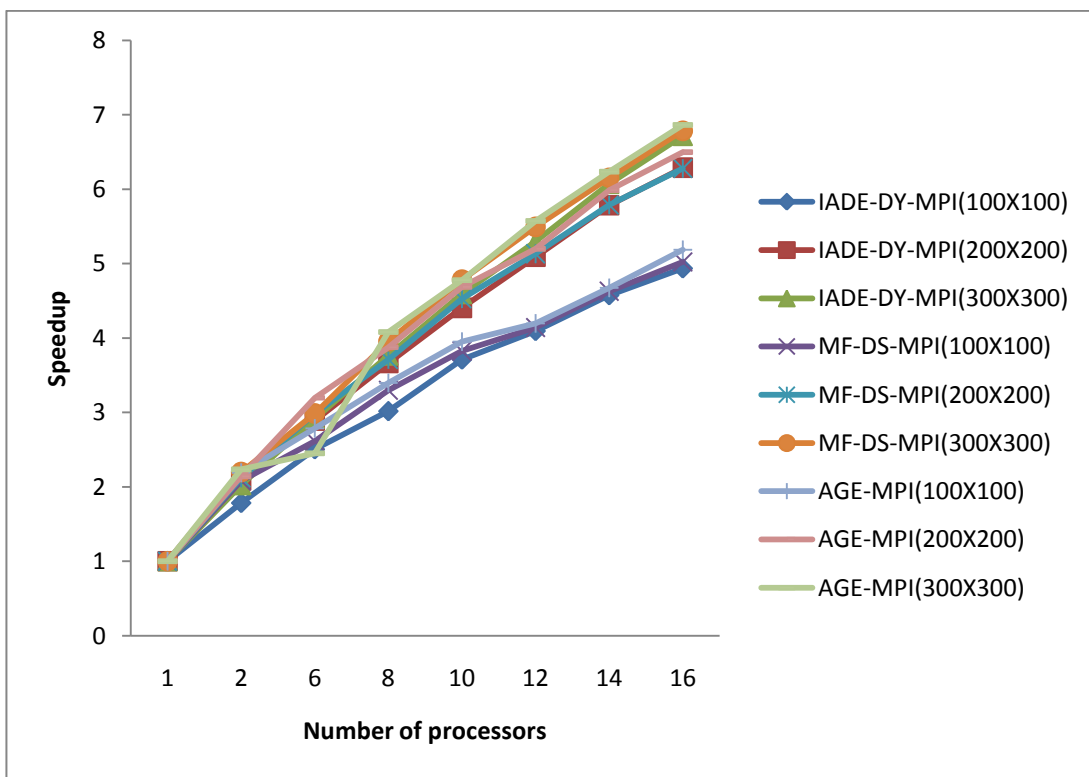


Fig. 6.15 Speedup for 100x100 to 300x300 meshes with MPI (2-D Bio-Heat)

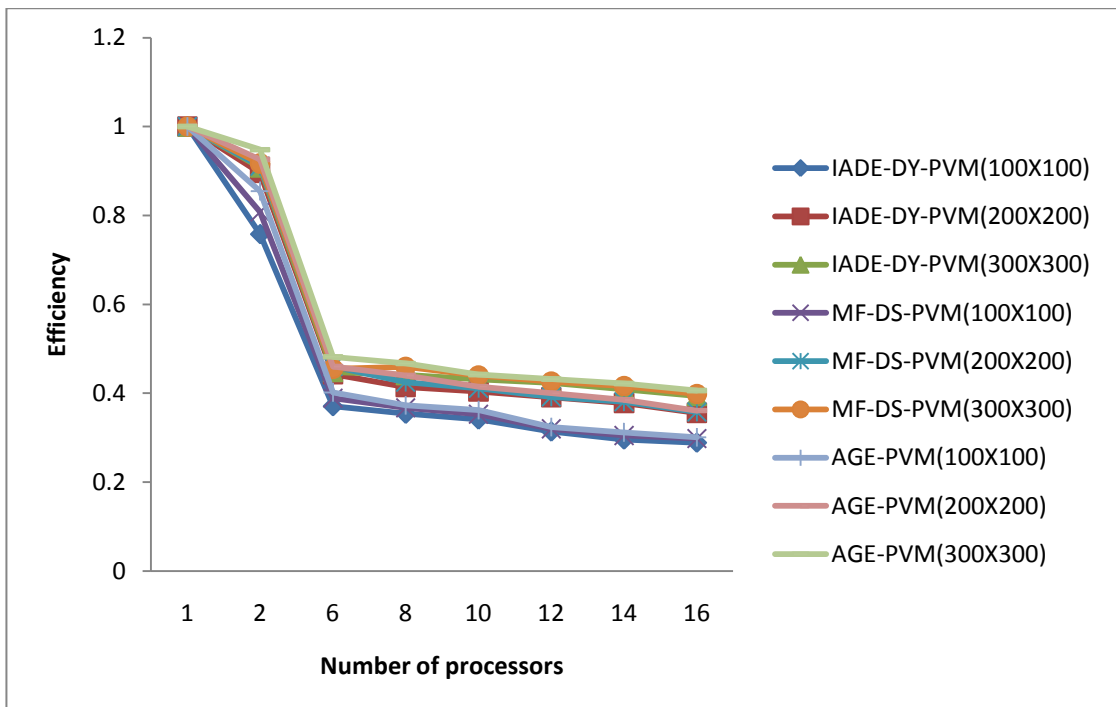


Fig. 6.16 Efficiency for 100x100 to 300x300 meshes with PVM (2-D Parabolic)

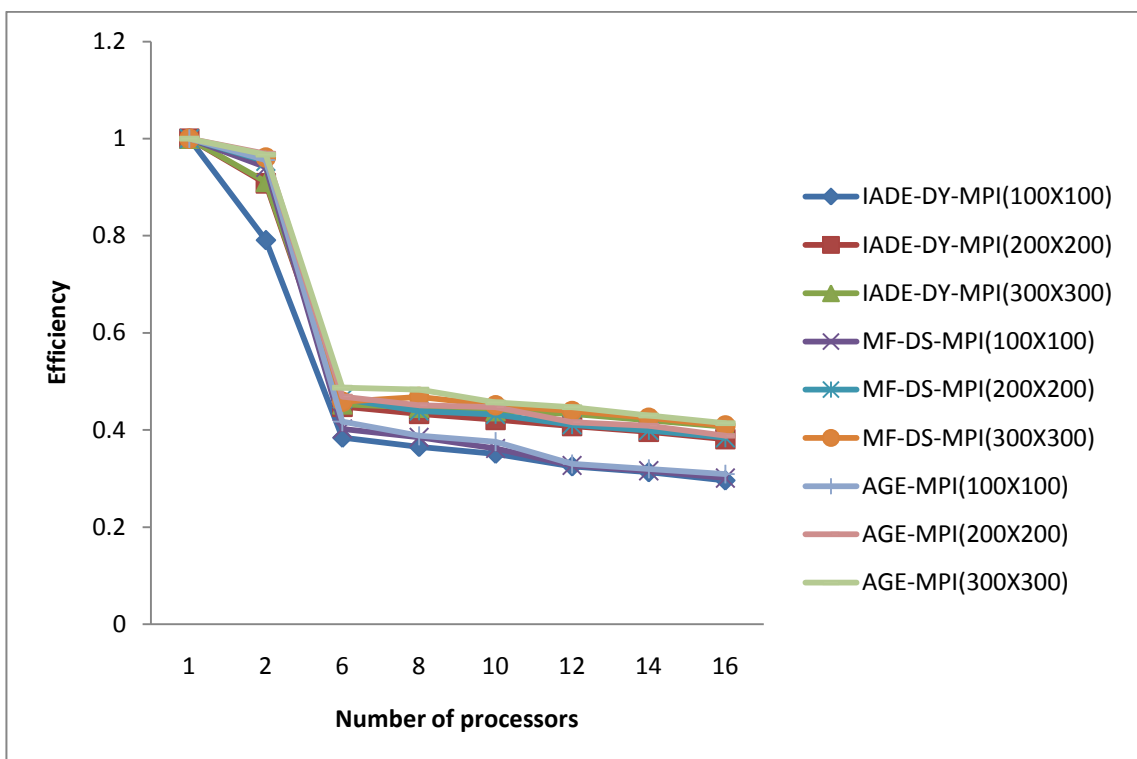


Fig. 6.17 Efficiency for 100x100 to 300x300 meshes with MPI (2-D Parabolic)

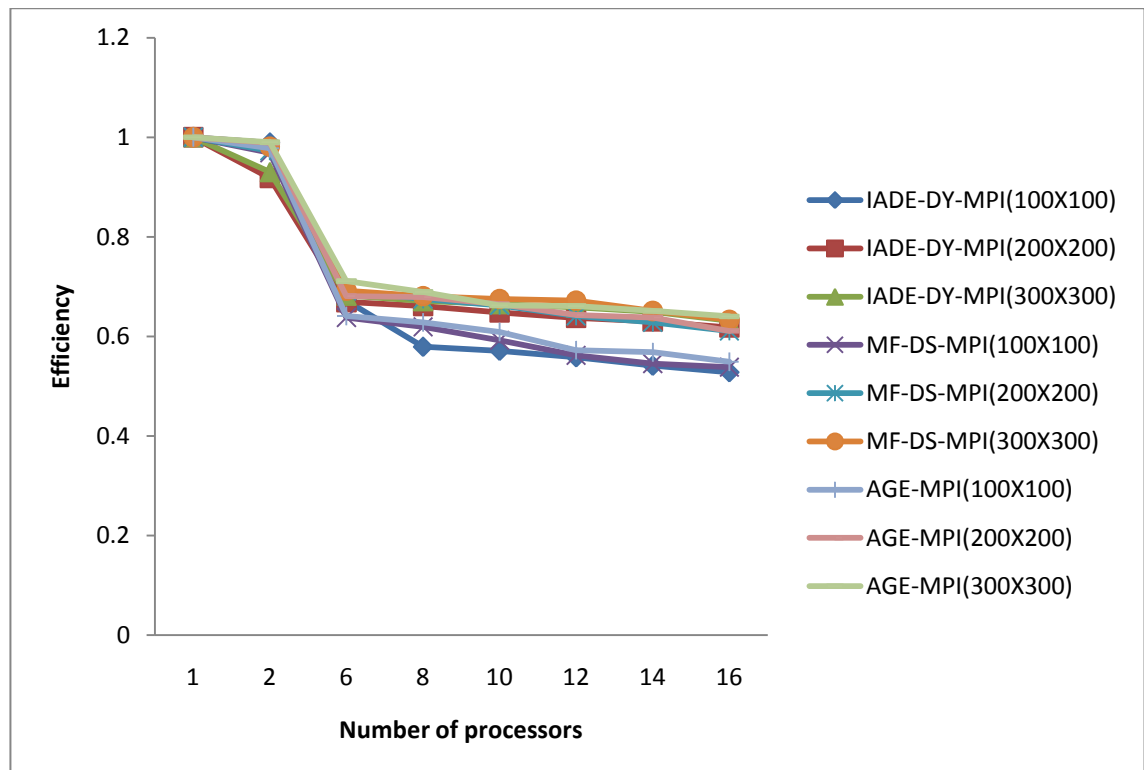


Fig. 6.18 Efficiency for 100x100 to 300x300 meshes with PVM (2-D Bio-Heat)

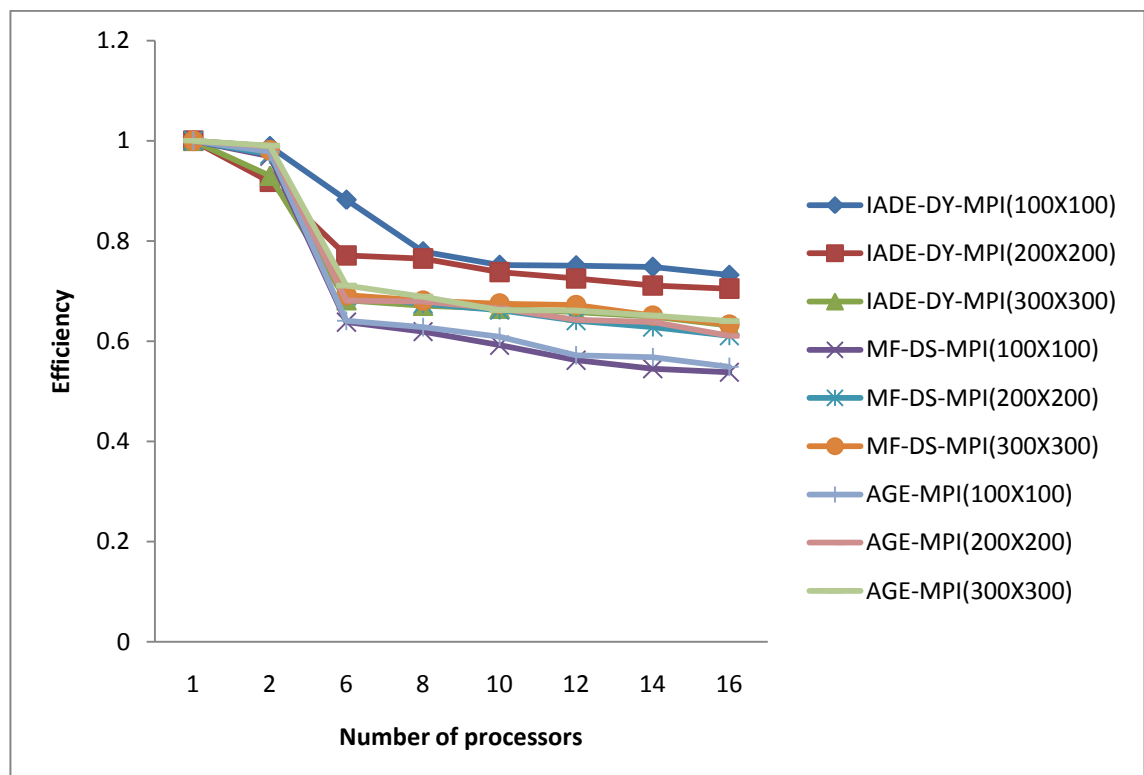


Fig. 6.19 Efficiency for 100x100 to 300x300 meshes with MPI (2-D Bio-Heat)

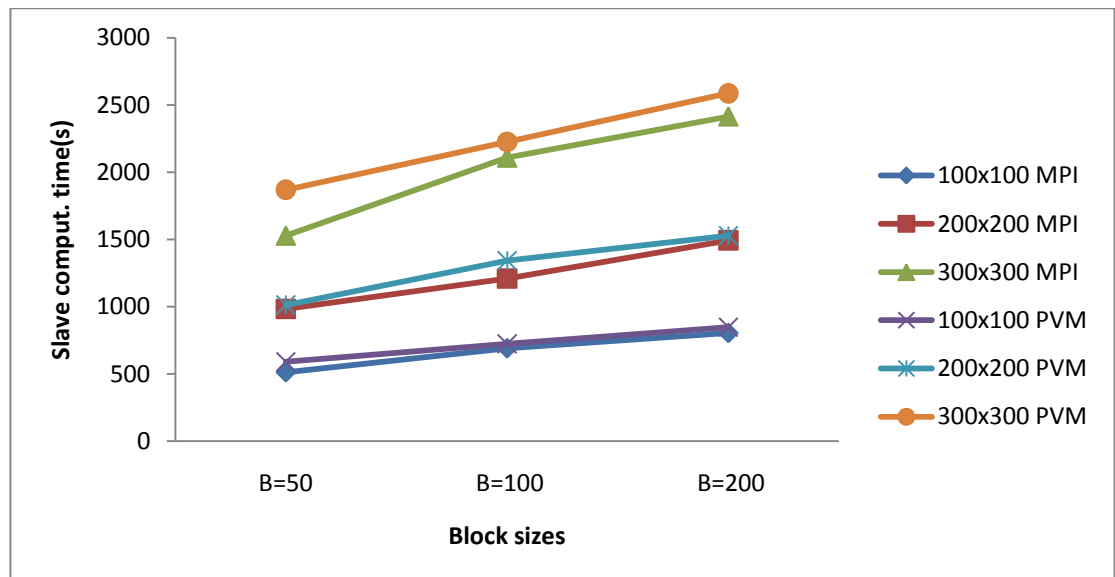


Fig.6.20 Slave computational time for various block sizes (2-D Parabolic MPI/PVM)

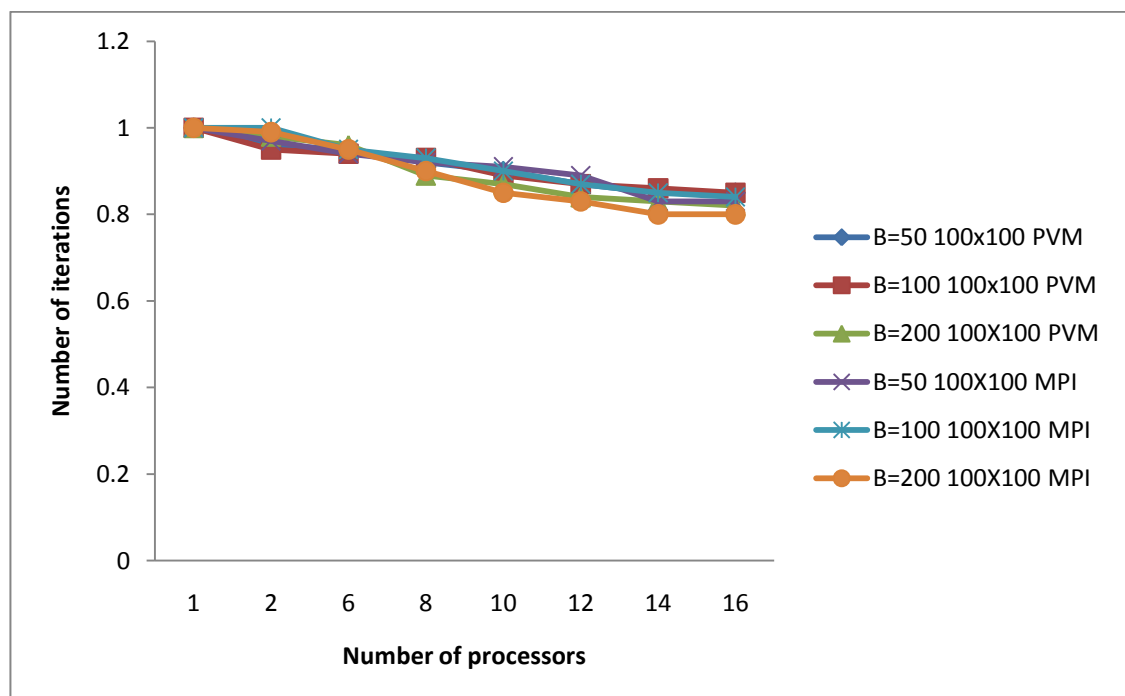


Fig.6.21 Number of iterations versus block sizes for 100x100 MPI and PVM

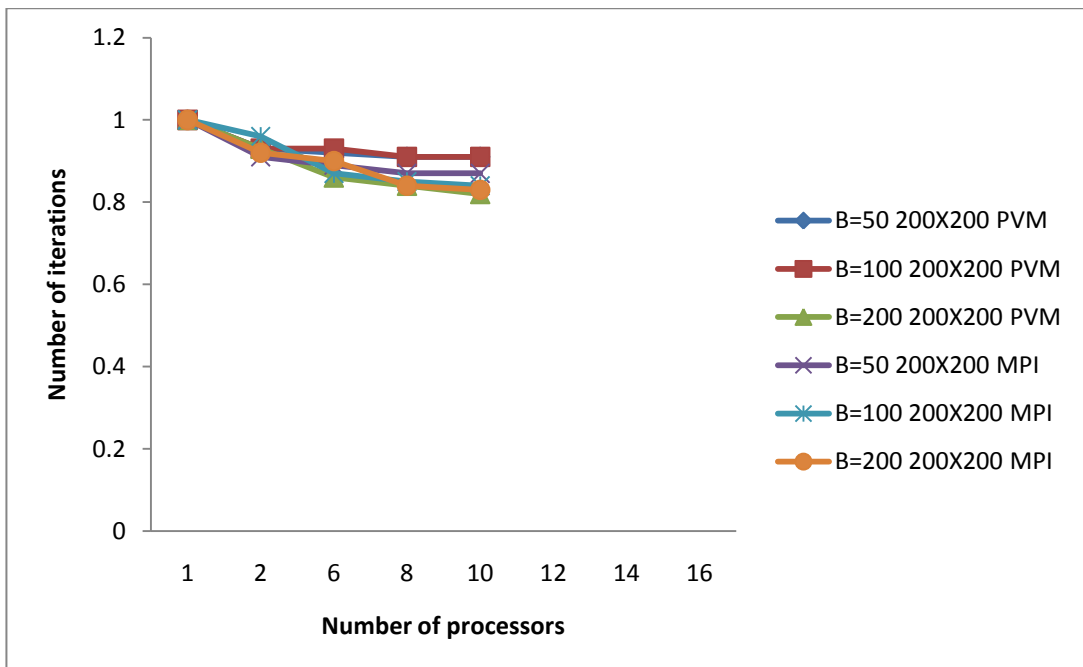


Fig.6.22 Number of iterations versus block numbers for 200x200 PVM and MPI.

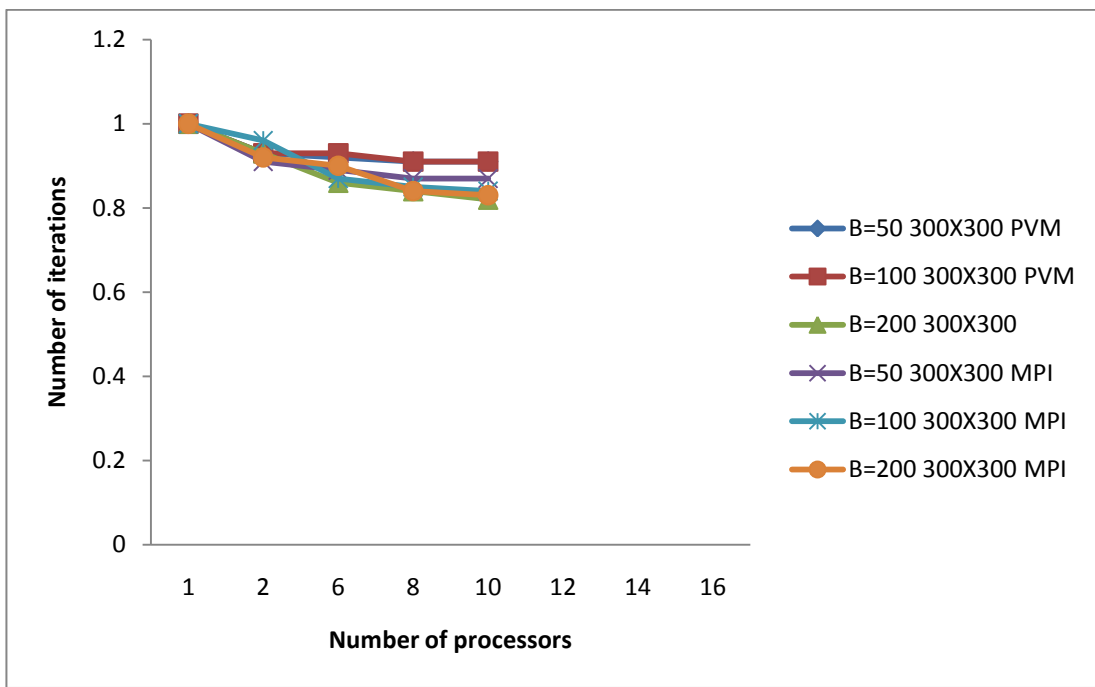


Fig.6.23 Number of iterations versus block numbers for 300x300 PVM AND MPI.

6.6 Sequential Computational Results for 1-D Telegraph Equation

To demonstrate the implicit formulation on the Telegraph Equation and using the *LU* algorithm to solve the resulting linear system and also using the IAGE-MF to solve the

solution of the linear system, numerical tests have been carried out. The values of the physical properties in our test case are chosen in such a way that LC , $(RC + GL)$, are equal to one. Table 6.21 shows the various numerical results on Eq. (4.1) with the boundary condition and initial condition posed as:

$$\frac{\partial^2 U}{\partial x^2} = LC \frac{\partial^2 U}{\partial t^2} + (RC + GL) \frac{\partial U}{\partial t} + RGU, \quad 0 \leq x \leq 1, 0 \leq t \leq 1$$

$$\left. \begin{array}{l} U(0,t) = 0 \\ U(1,t) = 100 \end{array} \right\} \quad t \geq 0 \quad (6.11)$$

and

$$\begin{aligned} U(x,0) &= \sin(\pi x) \quad 0 \leq x \leq 1 \\ U_t(x,0) &= \sin(\pi x) \quad 0 \leq x \leq 1 \end{aligned} \quad (6.12)$$

The exact solution is given by

$$U(x,y,t) = e^{-\pi t} \sin(\pi x).$$

Table 6.21 Numerical results for 1-D Telegraph Equation with various schemes

<i>Method</i>	<i>Av. Abs.</i>	<i>RMS</i>	<i>It</i>	Δx	Δt	λ	<i>t</i>	<i>eps</i>
<i>Err.</i>								
3-L IMP								
	6.3×10^{-4}	3.7×10^{-4}	5	1×10^{-1}	5×10^{-3}	5×10^{-1}	2.5×10^{-1}	1×10^{-4}
IADE-MF	3.2×10^{-4}	2.3×10^{-7}	3	1×10^{-1}	5×10^{-3}	5×10^{-1}	2.5×10^{-1}	1×10^{-4}

6.7 Parallel Results for 1-D Telegraph Equation

The CPU time for the master task and the data communication is constant for a given grid size and sub-domain. Therefore, the task in the inner loop should be made as large as possible to maximize the efficiency. The speedup and efficiency obtained for 300 mesh sizes for the MPI and PVM implementation on 1-D Telegraph Equation is listed in Table 6.22 for 100 iterations. In the Table, we also listed the elapsed time for the

master task, T_w , the master CPU time, T_m , the average slave computational time, T_{sc} , and the slave data communication time, T_{sd} , all in seconds.

Table 6.22: 300 mesh size using two schemes (1-D Telegraph)

PVM						MPI				
Scheme	N	T_w	T_m	T_{sd}	T_{sc}	S_{par}	E_{par}	N	S_{par}	E_{par}
	1	476.9	15.2	3.6	270.8	1.000	1.000	1	1.000	1.000
	2	318.5	14.8	3.8	142.6	1.797	0.899	2	1.912	0.956
	8	189.9	14.6	3.6	36.3	5.314	0.664	8	5.486	0.686
Imp	10	163.7	14.6	3.6	28.21	6.240	0.624	10	6.410	0.641
	14	149.9	14.6	3.6	23.99	6.864	0.490	14	6.928	0.495
	16	136.8	14.6	3.6	21.6	7.108	0.444	16	7.211	0.451
	1	529.8	29.5	7.4	361.8	1.000	1.000	1	1.000	1.000
	2	412.3	28.2	7.4	171.0	1.930	0.965	2	2.246	0.968
	8	218	28.2	7.3	23.69	6.736	0.842	8	6.813	0.852
IADE-	10	199.5	28.2	7.3	14.78	7.930	0.793	10	8.113	0.811
MF										
	14	178.1	28.2	7.3	11.64	8.458	0.604	14	9.004	0.688
	16	166.2	28.2	7.3	10.52	8.924	0.558	16	9.325	0.653

Table 6.23 Effectiveness of the various schemes with PVM and MPI for 300 mesh size

(1-D Telegraphic case)

	N	PVM $T(s)$	L_n	MPI $T(s)$	L_n
	1	289.6	0.35	261.2	0.38
	2	161.1	0.56	136.6	0.70
IMP	8	54.50	1.22	47.62	1.44
	10	46.41	1.34	40.76	1.58
	14	42.19	1.16	37.71	1.31
	16	40.74	1.09	36.23	1.24
	1	398.7	0.25	371.6	0.27
IADE-	2	206.58	0.47	165.5	0.59
MF					
	8	59.19	1.42	54.54	1.56
	10	50.28	1.58	45.80	1.77
	14	47.4	1.28	41.27	1.67
	16	44.68	1.25	39.85	1.64

Table 6.24 Improvement of performance for two schemes on 1-D Telegraph Equation.

Size	N	T(s)		T(s)		PVM(%)	MPI(%)
		PVM Imp	IADE- MF	MPI Imp	IADE- MF	Improvement	Improvement
	1	289.6	398.7	261.24	371.6	27.4	29.7
	2	161.1	206.6	136.6	165.5	22	17.4
300 x 300	8	54.50	59.19	47.62	54.54	7.9	12.7
	10	46.41	50.28	40.76	45.80	7.7	11.0
	14	42.19	47.14	37.71	41.27	10.5	8.6
	16	40.74	44.68	36.23	39.85	8.8	9.1

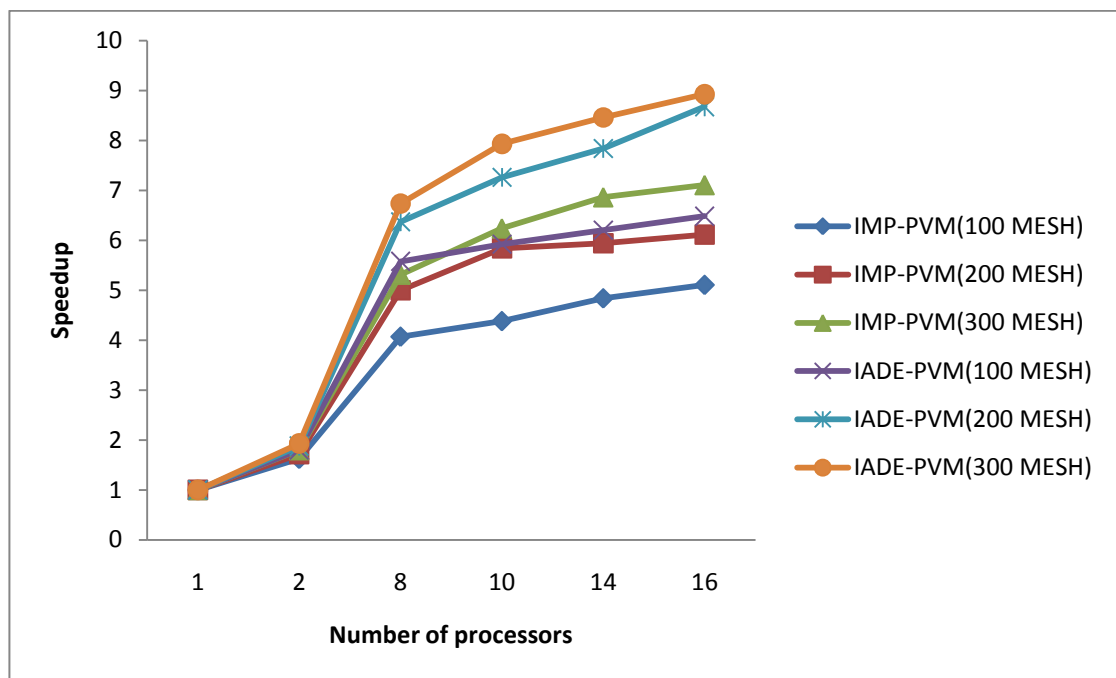


Fig. 6.24 1-D Telegraph Speedup of various mesh sizes with PVM

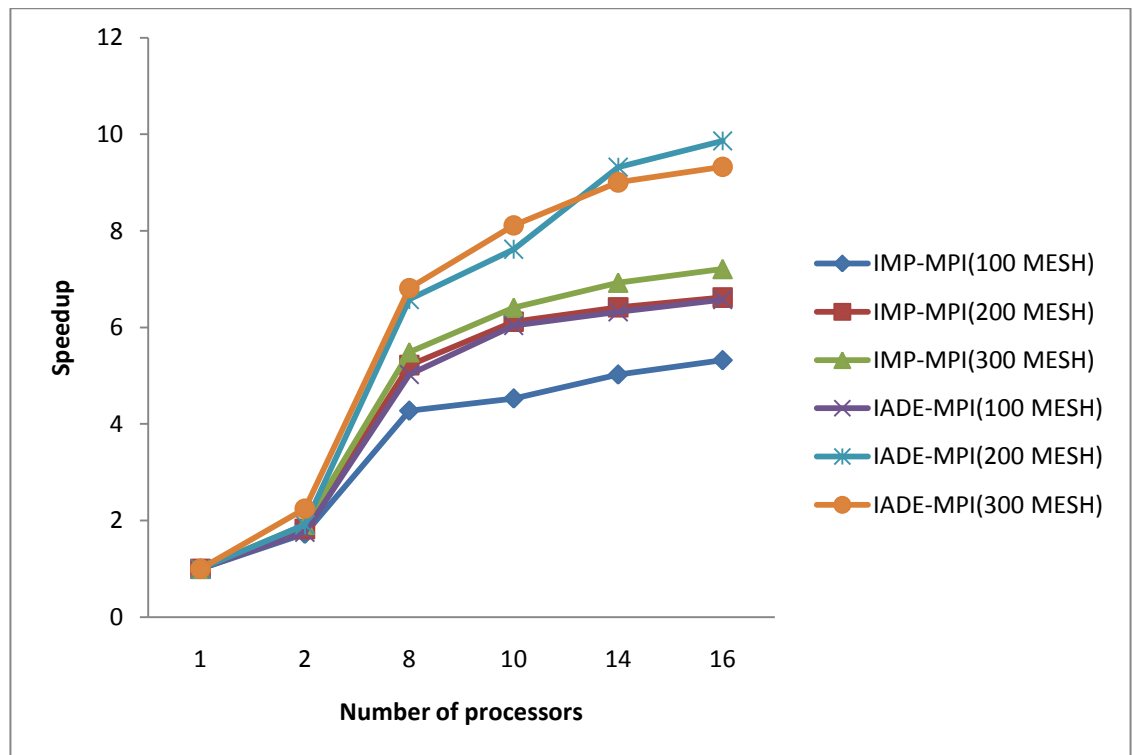


Fig. 6.25 1-D Telegraph Speedup of various mesh sizes with MPI

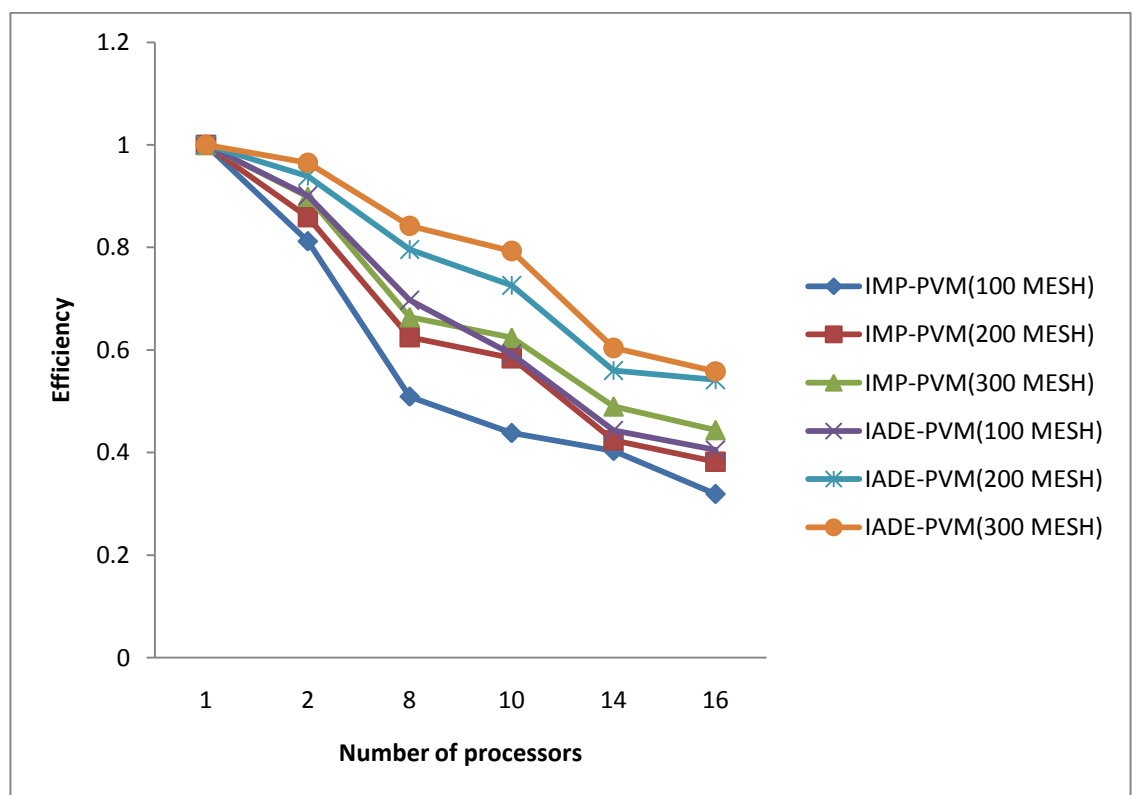


Fig. 6.26 1-D Telegraph Efficiency of various mesh sizes with PVM

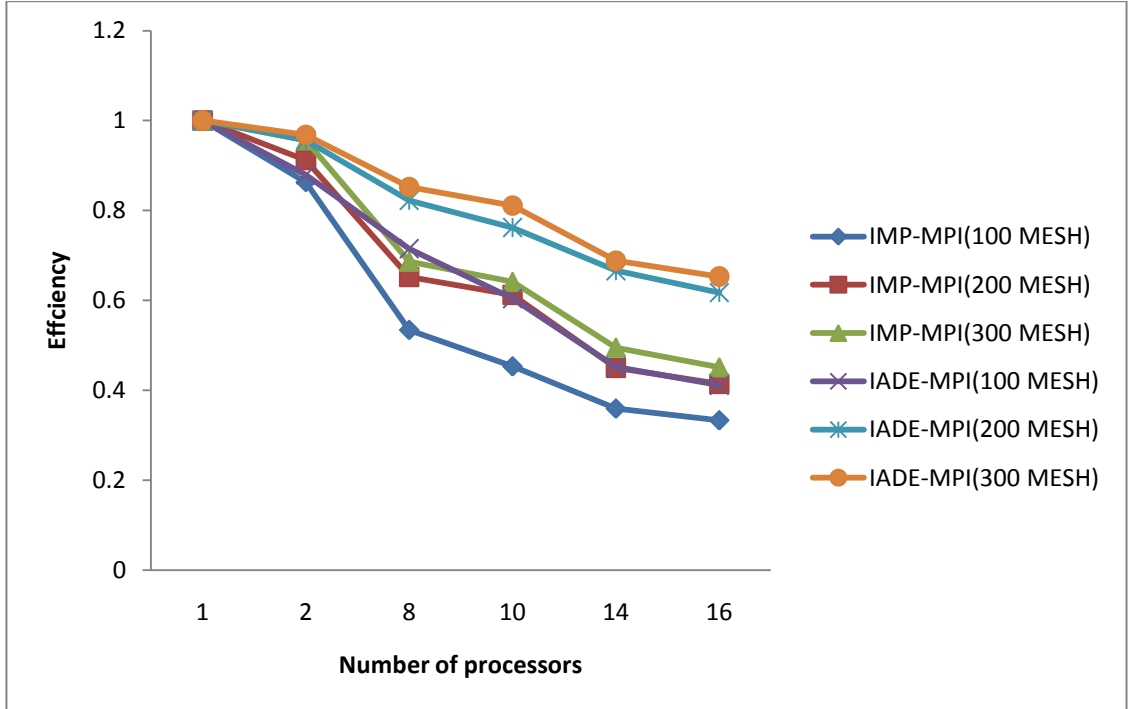


Fig. 6.27 1-D Telegraph Efficiency of various mesh sizes with MPI

6.8 Sequential Results for 2-D Telegraph Equation

We evaluate the various schemes discussed in Chapter 4 on the Telegraphic Equation with the values of the physical properties in our test case chosen in such a way that LC, $(RC + GL)$, are equal to one. The numerical solutions are graphed in Fig. 6.28 for average of absolute errors and in Fig. 6.29 for the root mean squares (rms), with the values $\lambda = 0.5$, $\Delta t = 0.05$, $\Delta x = 0.5$, $\Delta y = 0.5$, $r = 0.5$, and $\varepsilon = 10^{-4}$.

According to (Mohanty et. al. (1995)), Eq. (4.4) is considered with the boundary condition and initial condition posed as:

$$\frac{\partial^2 v}{\partial t^2} + a \frac{\partial v}{\partial t} = b \left(\frac{\partial^2 v}{\partial x^2} + \frac{\partial^2 v}{\partial y^2} \right) \quad 0 \leq x \leq 1, 0 \leq y \leq 1, t > 0$$

$$\left. \begin{array}{l} v(0, y, t) = 0 \\ v(1, y, t) = 100 \\ v(x, 0, t) = 0 \\ v(x, 1, t) = 100 \end{array} \right\} \quad t \geq 0 \quad (6.13)$$

$$v(x, y, 0) = e^{xy}, \quad (6.14)$$

Exact solution: $v(x, y, t) = e^{xy-t}$

Table 6.25: The absolute errors of the schemes solution to the 2-D telegraph equation
 $\lambda = 0.5, \Delta t = 0.05, \Delta x = 0.5, \Delta y = 0.5, r = 0.5, \text{eps} = 10^{-4}$.

<i>t</i>	<i>method</i>	0.5	1.0	1.5	2.0
0.5	<i>ADI</i>	0.2341873E-4	0.1934786E-4	0.1637992E-4	0.1466718E-4
	<i>IADE-DY</i>	0.3452816E-5	0.2134631E-5	0.1946342E-5	0.1784694E-5
	<i>MF-DS</i>	0.5568412E-6	0.2675781E-6	0.2045187E-6	0.1845328E-6
1.0	<i>ADI</i>	0.6876821E-3	0.5284172E-3	0.8246118E-3	0.7124638E-3
	<i>IADE-DY</i>	0.4790324E-4	0.3467814E-4	0.5841241E-3	0.5249378E-4
	<i>MF-DS</i>	0.1125567E-5	0.1011284E-5	0.5784373E-6	0.4125481E-5
1.5	<i>ADI</i>	0.6978924E-3	0.8246283E-3	0.7921183E-3	0.5621836E-3
	<i>IADE-DY</i>	0.5671284E-3	0.6794285E-3	0.6257897E-3	0.3478971E-3
	<i>MF-DY</i>	0.3895562E-4	0.6124373E-4	0.4825721E-4	0.2568478E-4
2.0	<i>ADI</i>	0.5256482E-2	0.5086438E-2	0.4123464E-2	0.7984769E-2
	<i>IADE-DY</i>	0.3784672E-2	0.3467942E-2	0.2452894E-2	0.5947825E-2
	<i>MF-DY</i>	0.1845857E-3	0.1457824E-3	0.1257824E-3	0.5486392E-3

Table 6.26: The average of absolute errors, root mean squares of 2-D telegraph
 $\lambda = 0.5, \Delta t = 0.05, \Delta x = 0.5, \Delta y = 0.5, r = 0.5, \text{eps} = 10^{-4}$.

		<i>Av. of</i> <i>absolute errors</i>	<i>Root mean</i> <i>square</i>
<i>t</i>	<i>method</i>		
0.5	<i>ADI</i>	1.84534225E-5	3.515511374E-10
	<i>IADE-DY</i>	2.32962075E-6	2.345196769E-11
	<i>MF-DS</i>	3.03367711E-7	1.143876036E-13
1.0	<i>ADI</i>	6.88293725E-4	1.218937027E-5
	<i>IADE-DY</i>	1.79799815E-4	8.686346373E-8
	<i>MF-DS</i>	1.71019232E-6	4.910944898E-12
1.5	<i>ADI</i>	7.19205651E-4	5.276418591E-7
	<i>IADE-DY</i>	5.55060921E-4	3.239757124E-7
	<i>MF-DY</i>	4.35353352E-5	2.064200259E-9
2.0	<i>ADI</i>	5.61278825E-3	3.356548647E-5
	<i>IADE-DY</i>	3.91333325E-3	1.693591877E-5
	<i>MF-DY</i>	2.51197425E-4	3.721505727E-7

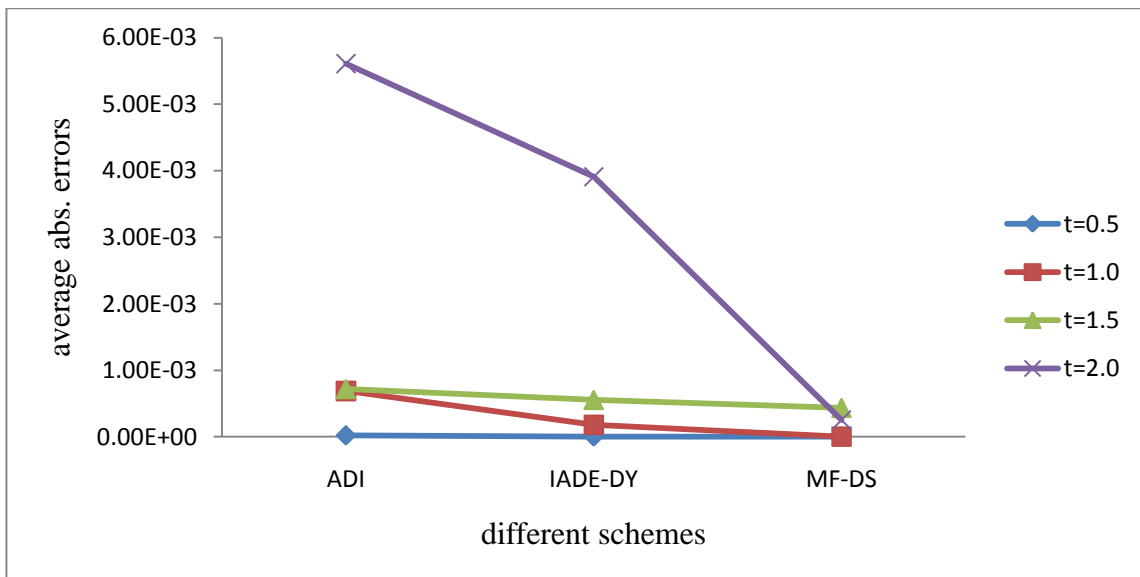


Fig. 6.28 average abs. errors for 2-D Telegraph Equation

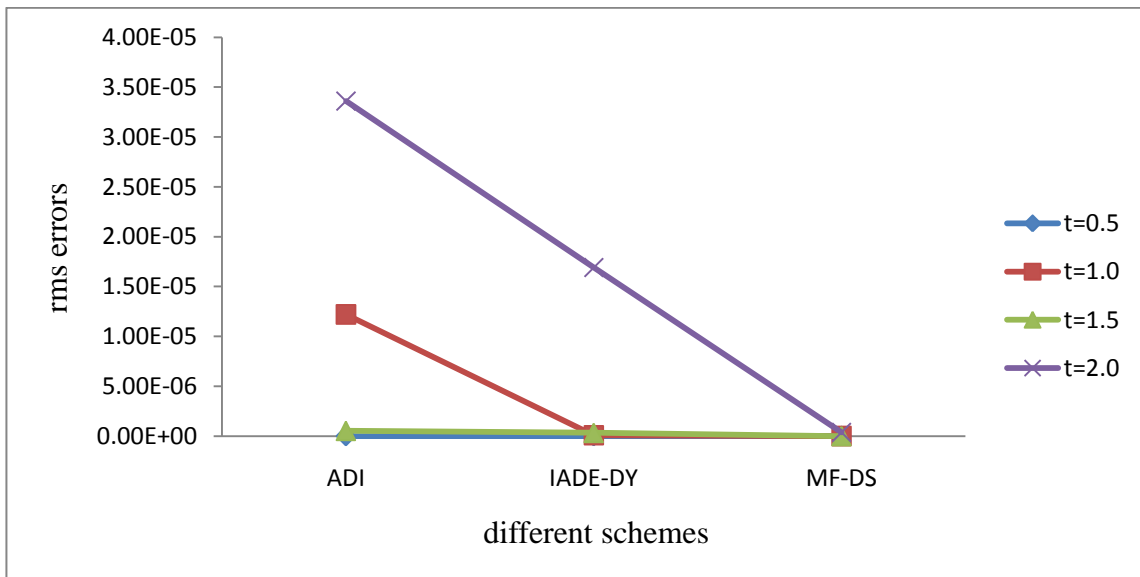


Fig. 6.29 rms errors for 2-D Telegraph Equation

6.9 Parallel Results for 2-D Telegraph Equation

The speedup and efficiency obtained for various schemes with 300 x 300 grid sizes for PVM and MPI implementation are listed in the Table below for 2-D Telegraph case.

Table 6.27: 300 x 300 meshes using three schemes

		PVM				MPI			
Scheme	N	T_w	T_m	T_{sd}	S_{par}	E_{par}	N	S_{par}	E_{par}
ADI	1	699.1	31.4	9.3	1.000	1.000	1	1.000	1.000
	2	621.6	31.2	9.1	1.882	0.941	2	1.896	0.948
	8	496.9	31.2	9.1	6.976	0.872	8	7.080	0.885
	10	438.5	31.2	9.1	8.48	0.848	10	8.550	0.855
	14	325.4	31.2	9.1	11.214	0.801	14	11.452	0.818
	16	299.3	31.2	9.1	12.624	0.789	16	12.752	0.797
<hr/>									
IADE	1	793.8	35.6	10.7	1.000	1.000	1	1.000	1.000
	2	658.4	35.5	10.4	1.906	0.953	2	1.922	0.961
	8	535.7	35.5	10.4	7.048	0.881	8	7.144	0.893
	10	499.2	35.5	10.4	8.560	0.856	10	8.620	0.862
	14	321.6	35.5	10.4	11.368	0.812	14	11.606	0.829
	16	293.7	35.5	10.4	12.72	0.795	16	13.072	0.817
<hr/>									
MF-DS	1	828.4	41.8	11.5	1.000	1.000	1	1.000	1.000
	2	696.9	41.6	11.4	1.924	0.962	2	1.946	0.973
	8	562.5	41.6	11.4	7.192	0.899	8	7.312	0.914
	10	512.3	41.6	11.4	8.750	0.875	10	8.81	0.881
	14	346.1	41.6	11.4	11.676	0.834	14	11.774	0.841
	16	311.8	41.6	11.4	13.136	0.821	16	13.36	0.835
<hr/>									

Table 6.28 Effectiveness of the various schemes with PVM and MPI for 300 x 300

mesh size (2-D Telegraphic case)

	N	PVM T(s)	L_n	MPI T(s)	L_n
ADI	1	1269	0.08	1148	0.09
	2	674.3	0.14	605.5	0.16
	8	181.9	0.48	162.2	0.55
	10	149.7	0.57	134.3	0.64
	14	113.2	0.71	100.2	0.82
	16	60.22	0.78	90.03	0.89
<hr/>					
IADE	1	1482	0.07	1378	0.07
	2	777.5	0.12	716.9	0.13
	8	210.3	0.42	192.9	0.46
	10	173.1	0.49	159.9	0.54
	14	130.4	0.62	118.7	0.70

	<i>16</i>	<i>116.5</i>	<i>0.68</i>	<i>105.4</i>	<i>0.76</i>
<i>MF-DS</i>	<i>1</i>	<i>1695</i>	<i>0.06</i>	<i>1528</i>	<i>0.07</i>
	<i>2</i>	<i>880.9</i>	<i>0.11</i>	<i>785.2</i>	<i>0.12</i>
	<i>8</i>	<i>235.7</i>	<i>0.38</i>	<i>208.9</i>	<i>0.44</i>
	<i>10</i>	<i>193.7</i>	<i>0.45</i>	<i>173.4</i>	<i>0.51</i>
	<i>14</i>	<i>145.2</i>	<i>0.57</i>	<i>129.8</i>	<i>0.65</i>
	<i>16</i>	<i>75.73</i>	<i>0.64</i>	<i>114.4</i>	<i>0.73</i>

Table 6.29 Performance improvement of different schemes for 300x300 mesh size on 2-

D Telegraphic Equation

<i>N</i>	<i>PVM</i>		<i>Time(s)</i>		%		<i>MPI</i>		<i>Time(s)</i>		%		
	<i>ADI</i>	<i>IADE</i>	<i>MF-DS</i>	<i>ADI+</i>	<i>IADE+</i>	<i>ADI</i>	<i>IADE</i>	<i>MF-</i>	<i>ADI+</i>	<i>IADE+</i>	<i>DS</i>	<i>IADE</i>	<i>MF-DS</i>
				<i>IADE</i>	<i>MF-DS</i>								
<i>1</i>	<i>126.9</i>	<i>1482</i>	<i>1695</i>	<i>14.4</i>	<i>12.6</i>	<i>1148</i>	<i>1378</i>	<i>1528</i>	<i>16.7</i>	<i>9.8</i>			
<i>2</i>	<i>674.3</i>	<i>777.5</i>	<i>880.9</i>	<i>13.3</i>	<i>11.7</i>	<i>605.5</i>	<i>716.9</i>	<i>785.2</i>	<i>15.5</i>	<i>8.7</i>			
<i>8</i>	<i>181.9</i>	<i>210.3</i>	<i>235.7</i>	<i>13.5</i>	<i>10.8</i>	<i>162.2</i>	<i>192.9</i>	<i>208.9</i>	<i>15.9</i>	<i>7.7</i>			
<i>10</i>	<i>149.7</i>	<i>173.1</i>	<i>193.7</i>	<i>13.6</i>	<i>10.6</i>	<i>134.3</i>	<i>159.9</i>	<i>173.4</i>	<i>16.0</i>	<i>7.8</i>			
<i>14</i>	<i>113.2</i>	<i>130.4</i>	<i>145.2</i>	<i>13.2</i>	<i>10.2</i>	<i>100.2</i>	<i>118.7</i>	<i>129.8</i>	<i>15.6</i>	<i>8.5</i>			
<i>16</i>	<i>100.5</i>	<i>116.5</i>	<i>129.0</i>	<i>13.7</i>	<i>9.7</i>	<i>90.03</i>	<i>105.42</i>	<i>114.4</i>	<i>14.6</i>	<i>7.8</i>			

Table 6.30 Slave computational time for 100 iterations as a function of block numbers for PVM (2-D Telegraphic case)

<i>NI x NJ</i>	<i>B = 50</i>	<i>B = 100</i>	<i>B = 200</i>
<i>100 x 100</i>	<i>196.8</i>	<i>243.7</i>	<i>308.2</i>
<i>200 x 200</i>	<i>584.3</i>	<i>698.1</i>	<i>719.9</i>
<i>300 x 300</i>	<i>1641.7</i>	<i>2017.5</i>	<i>2572.1</i>

Table 6.31 Slave computational time for 100 iterations as a function of block numbers for MPI (2-D Telegraph case)

<i>NI x NJ</i>	<i>B = 50</i>	<i>B = 100</i>	<i>B = 200</i>
<i>100 x 100</i>	<i>169.3</i>	<i>217.6</i>	<i>293.5</i>
<i>200 x 200</i>	<i>499.6</i>	<i>578.7</i>	<i>698.4</i>
<i>300 x 300</i>	<i>1599.8</i>	<i>1962.9</i>	<i>2132.7</i>

Table 6.32 The number of iteration to achieve a given tolerance of 10^{-4} for a grid of 100 x 100 PVM (2-D Telegraphic case)

N	B = 50	B = 100	B = 200
2	4421	4873	3184
8	4923	5214	3871
10	5118	5573	4126
14	5361	5571	4261
16	5361	5824	4328

Table 6.33 The number of iteration to achieve a given tolerance of 10^{-4} for a grid of 100 x 100 MPI (2-D Telegraphic case)

N	B = 50	B = 100	B = 200
2	4118	4610	2834
8	4583	4924	3118
10	4977	5328	3722
14	5185	5418	3971
16	5185	5421	4113

Table 6.34 The number of iteration to achieve a given tolerance of 10^{-4} for a grid of 200 x 200 PVM (2-D Telegraphic case)

N	B = 50	B = 100	B = 200
2	4962	5013	3628
8	5014	5338	3921
10	5311	5621	4218
14	5428	5681	4329
16	5428	5681	4478

Table 6.35 The number of iteration to achieve a given tolerance of 10^{-4} for a grid of 200 x 200 MPI (2-D Telegraphic case)

N	B = 50	B = 100	B = 200
2	4721	4816	3347
8	4926	5211	3767
10	5183	5487	3863
14	5219	5513	4108
16	5303	5513	4215

Table 6.36 The number of iteration to achieve a given tolerance of 10^{-4} for a grid of 300 x 300 PVM (2-D Telegraphic case)

<i>N</i>	<i>B = 50</i>	<i>B = 100</i>	<i>B = 200</i>
2	5824	5938	3729
8	6273	6397	3996
10	6318	6413	4321
14	6417	6528	4443
16	6417	6528	4527

Table 6.37 The number of iteration to achieve a given tolerance of 10^{-4} for a grid of 300 x 300 MPI (2-D Telegraphic case)

<i>N</i>	<i>B = 50</i>	<i>B = 100</i>	<i>B = 200</i>
2	5318	5324	3581
8	5821	5538	3897
10	5993	6119	3976
14	6086	6236	4274
16	6127	6312	4308

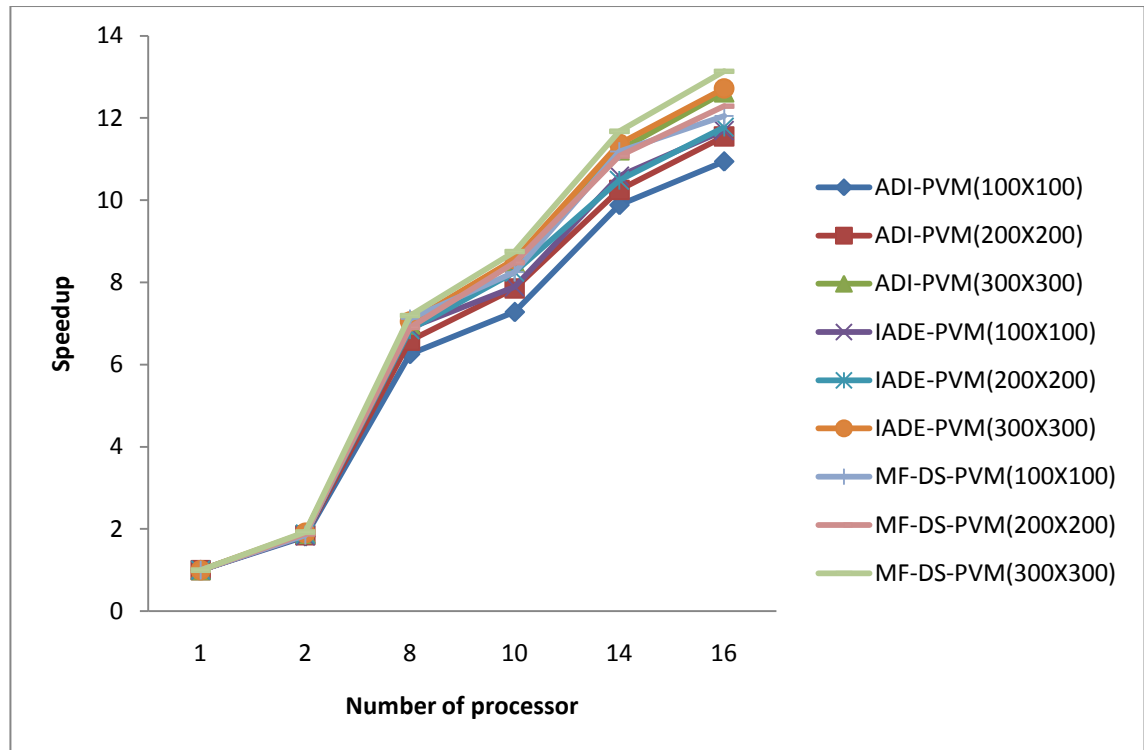


Fig. 6.30 Speedup of various mesh sizes with PVM for 2-D Telegraph

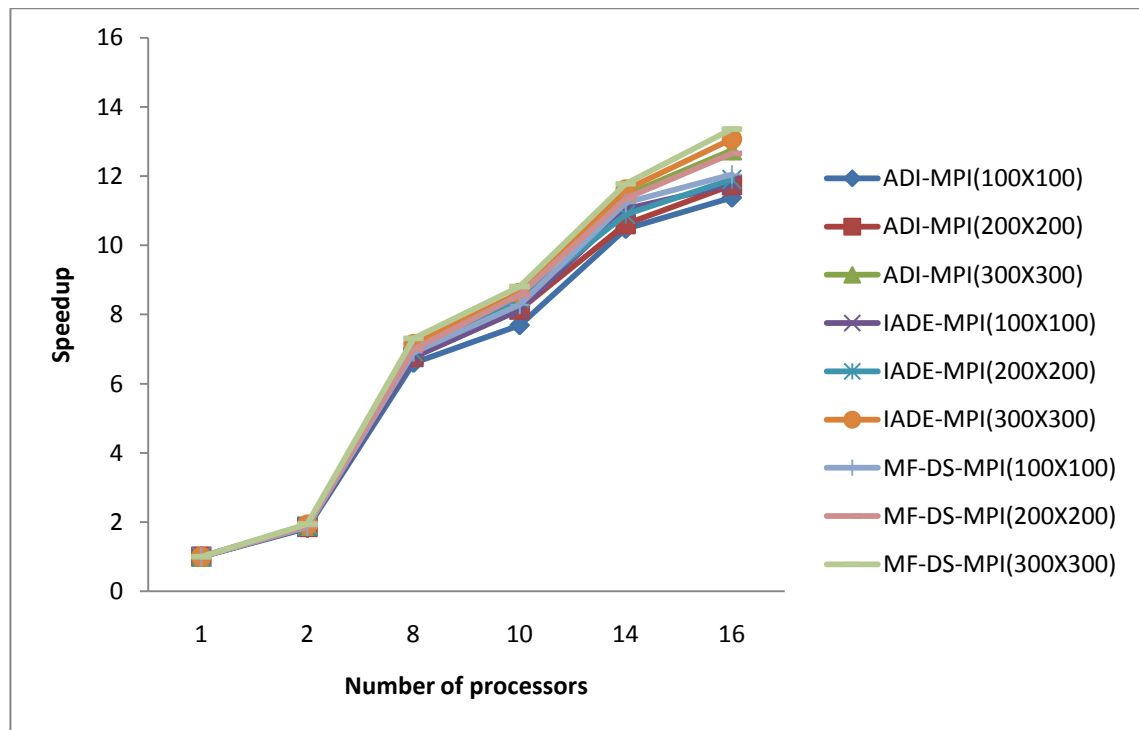


Fig. 6.31 Speedup of various mesh sizes with MPI for 2-D Telegraph

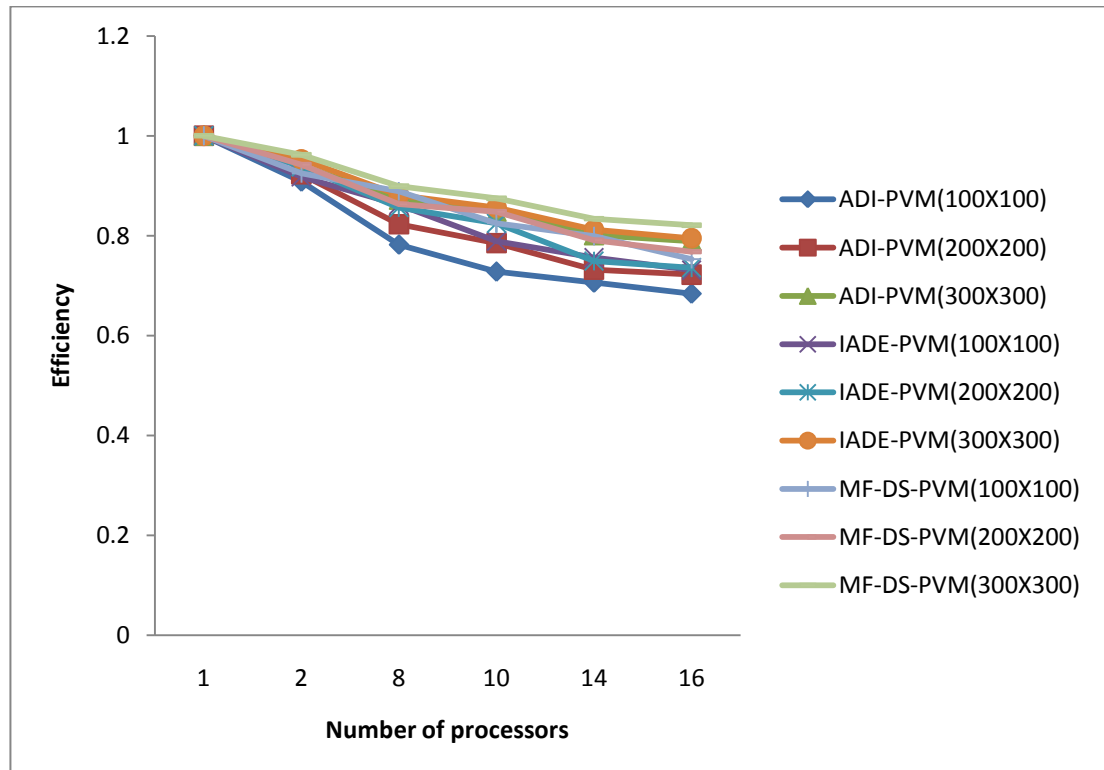


Fig. 6.32 Efficiency of various mesh sizes with PVM for 2-D Telegraph

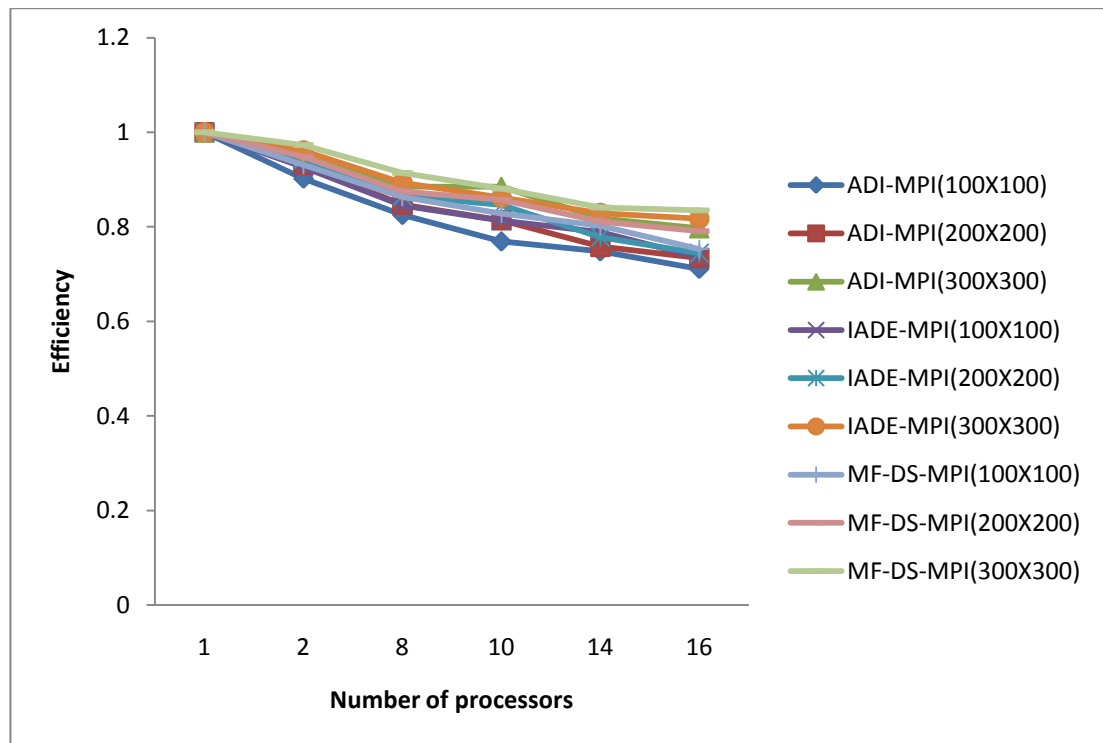


Fig. 6.33 Efficiency of various mesh sizes with MPI for 2-D Telegraph

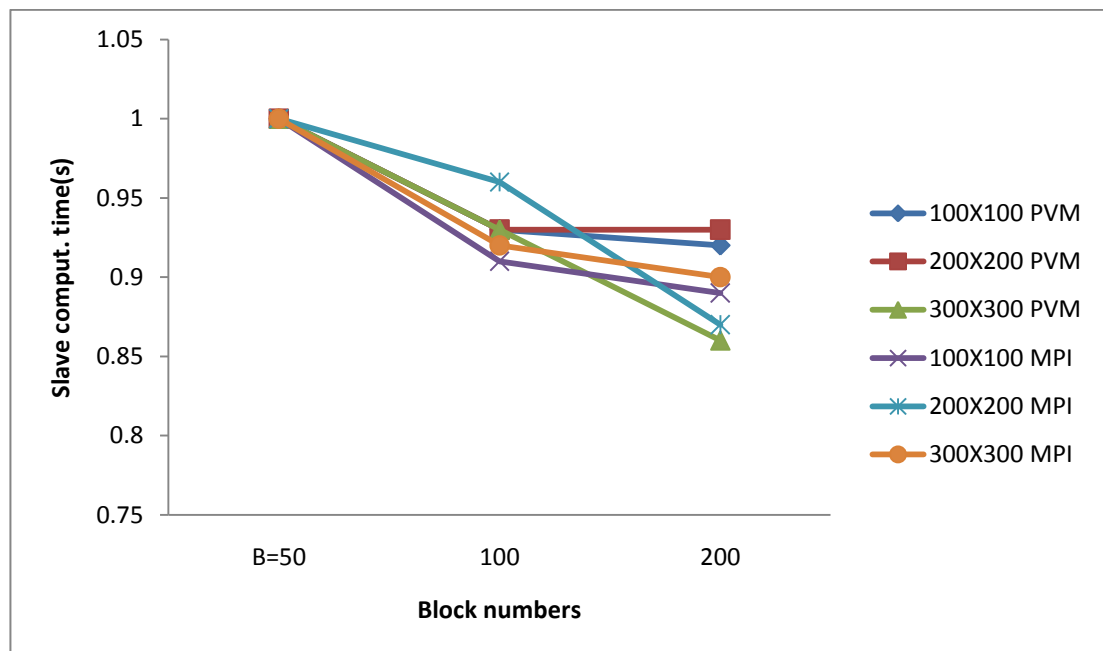


Fig.6.34 Slave computational time as function of block numbers for PVM and MPI

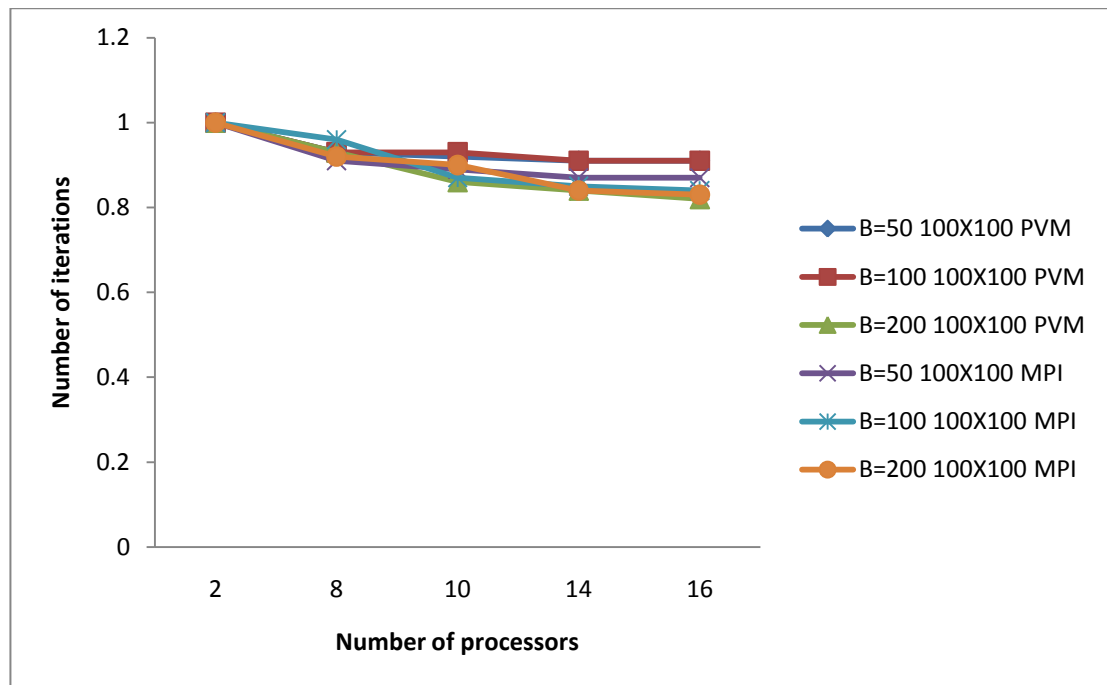


Fig.6.35. The number of iterations for different block sizes for 100 x 100 PVM & MPI

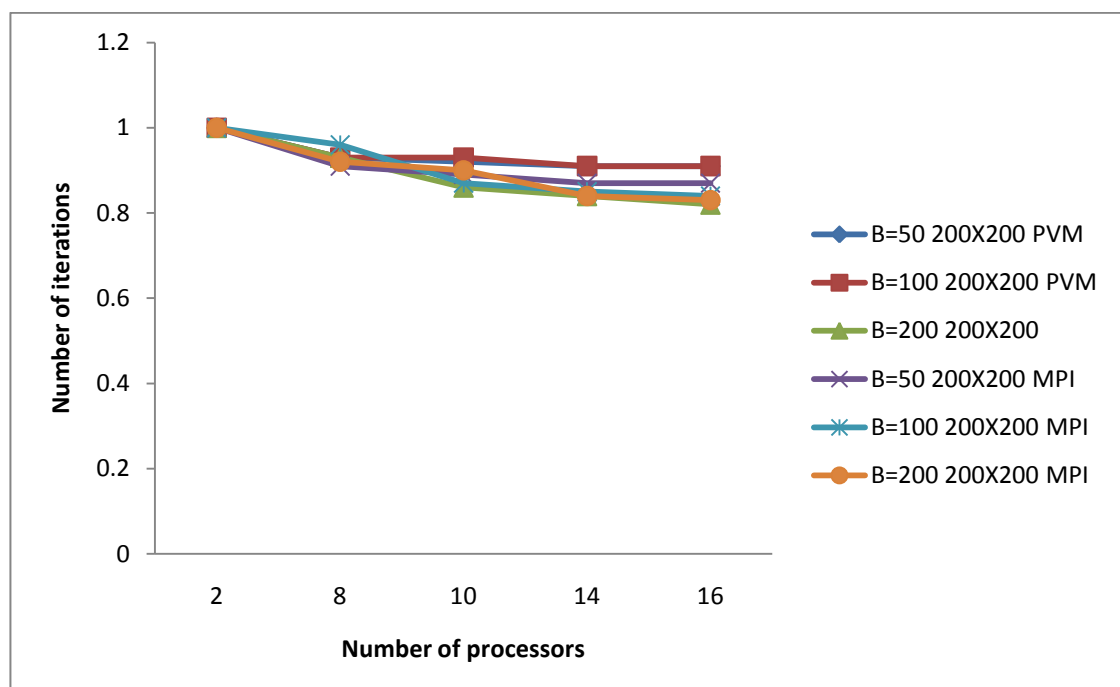


Fig.6.36. The number of iterations for different block sizes for 200x200 PVM & MPI

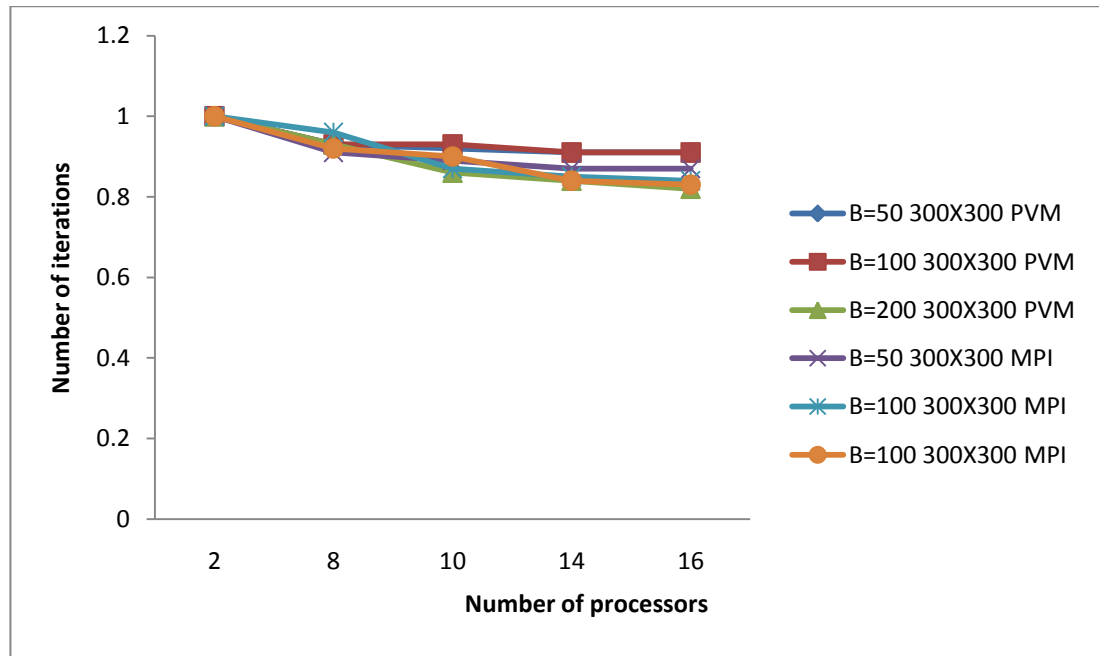


Fig.6.37 The number of iterations for different block sizes for 200x200 PVM & MPI

6.10 Sequential Results for 3-D Telegraph Equation

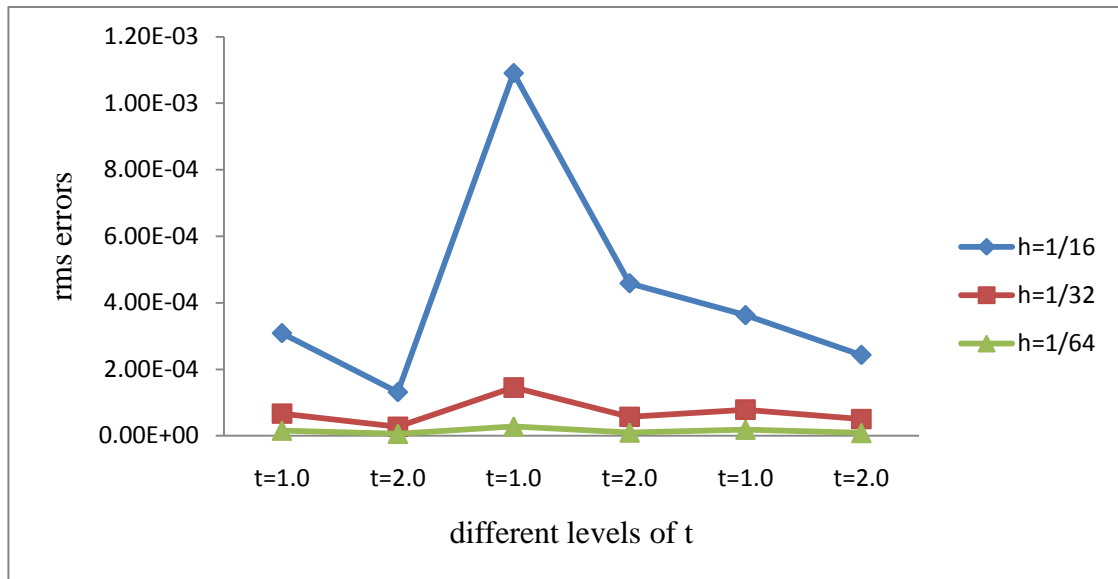
The 3-D ADI method outlined in this thesis is used to solve the proposed Eq. (5.1) in the region $0 < x, y, z < 1, t > 0$ whose exact solution is given by $v = e^{-t} \sin x \sin y \sin z$. The initial and boundary conditions and right hand side function can be obtained using the exact solution as a test procedure. Note that, the proposed difference scheme is a three level implicit scheme. To start any calculation, it is necessary to know the values of v at $t = k$ as well as $t = 0$. The accuracy of the solution at the grid points is determined by the root mean square (rms) errors.

Table 6.38: The RMS errors when $\lambda = 1.6$

<u>$R_x = 0.25, R_y = 0.5, R_z = 0.75$</u>			<u>$R_x = R_y = R_z = 1.0$</u>		<u>$R_x = 0.75, R_y = 0.5, R_z = 2.5$</u>	
h	$t = 1.0$	$t = 2.0$	$t = 1.0$	$t = 2.0$	$t = 1.0$	$t = 2.0$
1/16	0.3086(-03)	0.1311(-03)	0.1091(-02)	0.4586(-03)	0.3627(-03)	0.2430(-03)
1/32	0.6673(-04)	0.2714(-04)	0.1453(-03)	0.5738(-04)	0.7866(-04)	0.5010(-04)
1/64	0.1587(-04)	0.6384(-05)	0.2841(-04)	0.1007(-04)	0.1876(-04)	0.8802(-05)

 Table 6.39: The RMS errors when $\lambda = 3.2$

<u>$R_x = 0.5, R_y = 0.75, R_z = 1.0$</u>			<u>$R_x = R_y = R_z = 0.5$</u>		<u>$R_x = 0.5, R_y = 0.75, R_z = 1.0$</u>	
h	$t = 1.0$	$t = 2.0$	$t = 1.0$	$t = 2.0$	$t = 1.0$	$t = 2.0$
1/16	0.4100(-02)	0.1184(-02)	0.1853(-02)	0.1185(-02)	0.1189(-02)	0.6224(-03)
1/32	0.3068(-03)	0.1128(-03)	0.3403(-03)	0.1762(-03)	0.3061(-03)	0.1222(-03)
1/64	0.4792(-04)	0.1763(-04)	0.7473(-04)	0.3666(-04)	0.7441(-04)	0.2829(-04)


 Fig. 6.38 rms errors for $\lambda = 1.6$

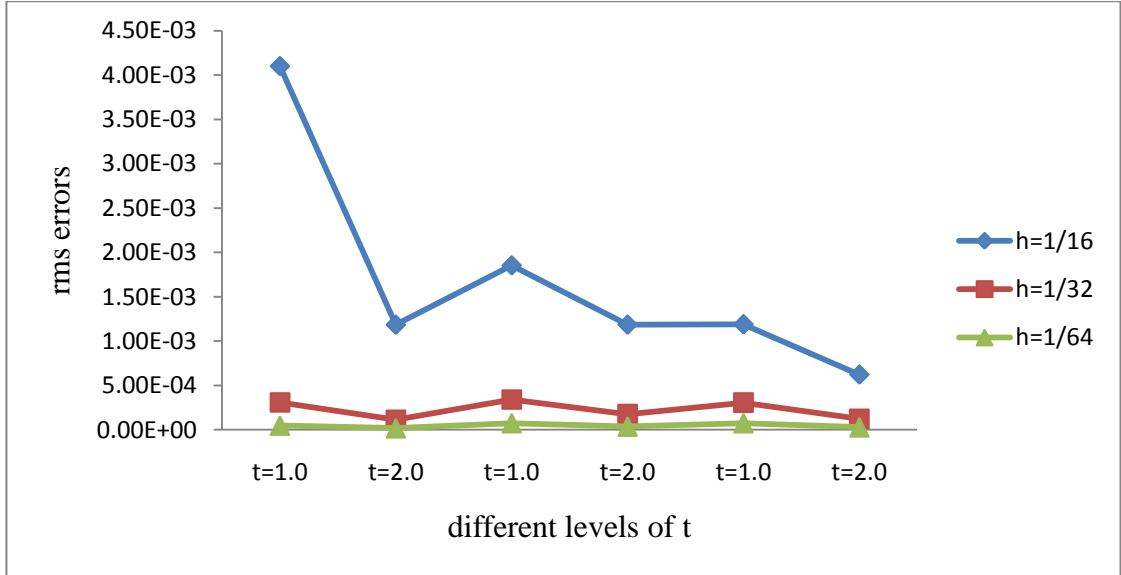


Fig.6.39 rms errors when $\lambda = 3.2$

Results for the problem using the 3-D ADI method showing the root mean square errors for $\lambda = 1.6$ and 3.2 , are given in Fig. 6.38 and Fig. 6.39, respectively.

6.11 Parallel Results for 3-D Telegraph Equation

The speedup and efficiency obtained for various schemes with 300×300 grid sizes for PVM and MPI implementation are listed in the Table and figures below for 3-D Telegraph case.

Table 6.40: $300 \times 300 \times 300$ meshes using three schemes

<i>Scheme</i>	<i>PVM</i>					<i>MPI</i>			
	<i>N</i>	<i>T_w</i>	<i>T_m</i>	<i>T_{sd}</i>	<i>S_{par}</i>	<i>E_{par}</i>	<i>N</i>	<i>S_{par}</i>	<i>E_{par}</i>
1		962.5	62.7	19.1	1.000	1.000	1	1.000	1.000
2		896.9	62.6	19	1.988	0.994	2	1.996	0.998
3D-ADI	8	728.1	62.6	19	8.213	0.978	8	7.928	0.991
	10	596.6	62.6	19	9.26	0.926	10	9.84	0.984
	14	499.3	62.6	19	12.866	0.919	14	13.608	0.972
	16	387.4	62.6	19	14.496	0.906	16	15.296	0.956

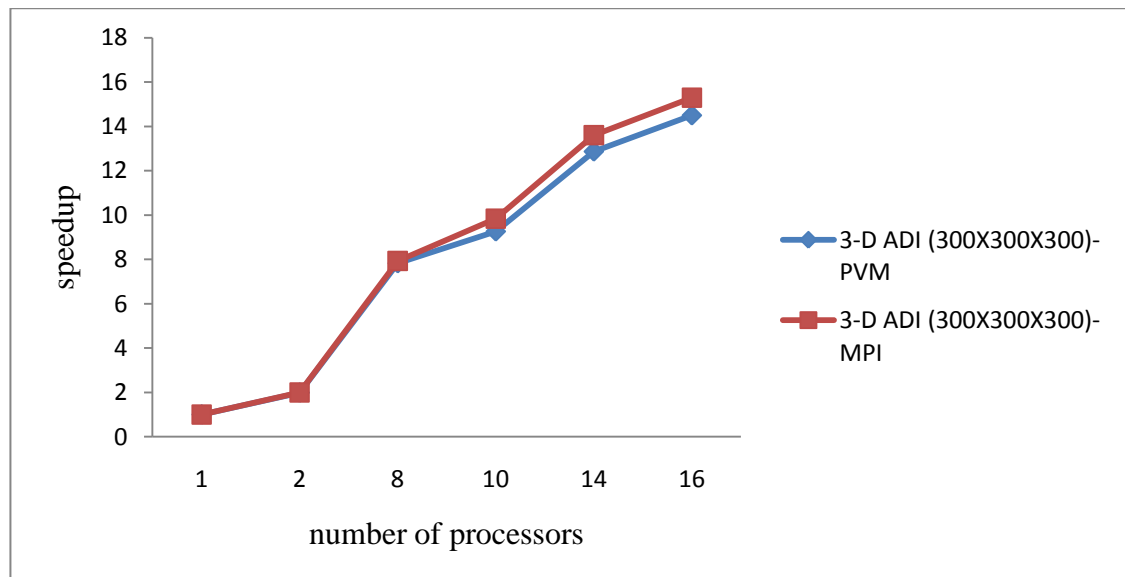


Fig. 6.40 Speedup for the 3-D ADI 300 x300x300 mesh sizes with PVM and MPI

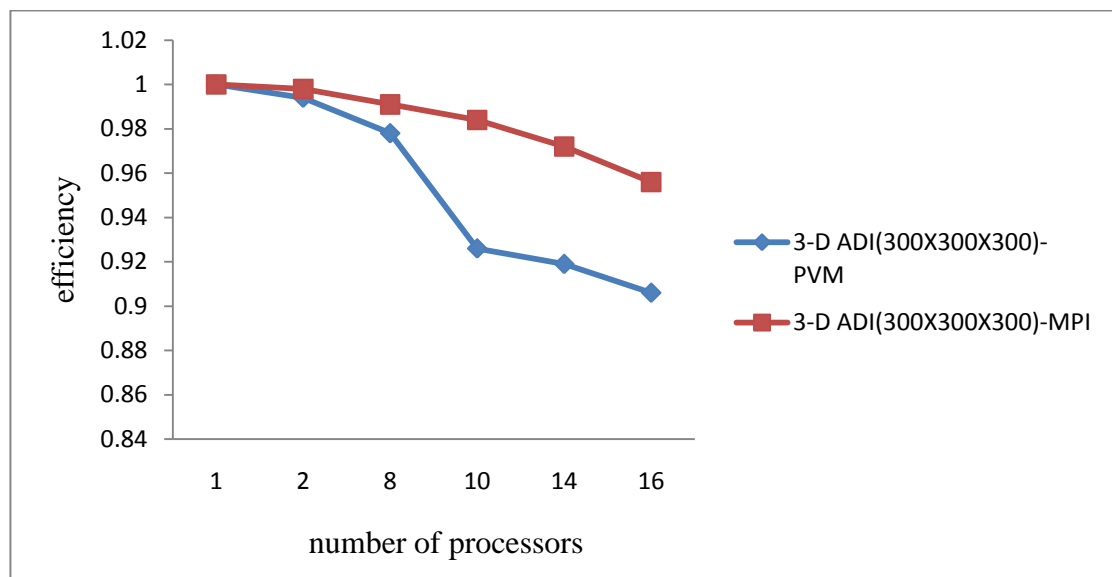


Fig 6.41 Efficiency for 3-D ADI (300x300x300) mesh sizes with PVM and MPI